Stem Cell Reports
Article

OPEN ACCESS

Endogenous WNT Signals Mediate BMP-Induced and Spontaneous Differentiation of Epiblast Stem Cells and Human Embryonic Stem Cells

Dorota Kurek,[1,2] Alex Neagu,[1,2] Melodi Tastemel,[1,2] Nesrin Tüysüz,[1,2] Johannes Lehmann,[1,2] Harmen J.G. van de Werken,[2] Sjaak Philipsen,[2] Reinier van der Linden,[1,2] Alex Maas,[2] Wilfred F.J. van IJcken,[3] Micha Drukker,[4] and Derk ten Berge[1,2,*]

[1]Erasmus MC Stem Cell Institute, Erasmus MC, Wytemaweg 80, 3015 CN Rotterdam, the Netherlands
[2]Department of Cell Biology, Erasmus MC, Wytemaweg 80, 3015 CN Rotterdam, the Netherlands
[3]Erasmus MC Center for Biomics, Erasmus MC, Wytemaweg 80, 3015 CN Rotterdam, the Netherlands
[4]Institute of Stem Cell Research, German Research Center for Environmental Health, Helmholtz Center Munich, Ingolstädter Landstraße 1, 85764 Neuherberg, Germany
*Correspondence: d.tenberge@erasmusmc.nl
http://dx.doi.org/10.1016/j.stemcr.2014.11.007

SUMMARY

Therapeutic application of human embryonic stem cells (hESCs) requires precise control over their differentiation. However, spontaneous differentiation is prevalent, and growth factors induce multiple cell types; e.g., the mesoderm inducer BMP4 generates both mesoderm and trophoblast. Here we identify endogenous WNT signals as BMP targets that are required and sufficient for mesoderm induction, while trophoblast induction is WNT independent, enabling the exclusive differentiation toward either lineage. Furthermore, endogenous WNT signals induce loss of pluripotency in hESCs and their murine counterparts, epiblast stem cells (EpiSCs). WNT inhibition obviates the need to manually remove differentiated cells to maintain cultures and improves the efficiency of directed differentiation. In EpiSCs, WNT inhibition stabilizes a pregastrula epiblast state with novel characteristics, including the ability to contribute to blastocyst chimeras. Our findings show that endogenous WNT signals function as hidden mediators of growth factor-induced differentiation and play critical roles in the self-renewal of hESCs and EpiSCs.

INTRODUCTION

Pluripotent stem cells can generate all cell types of the body and hold great potential for transplantation medicine and the study of early development. Pluripotency arises in the inner cell mass of blastocyst-stage embryos during formation of the epiblast, and both human and mouse blastocysts can give rise to pluripotent embryonic stem cells (ESCs). Differentiation of the pluripotent epiblast toward the primary germ layers occurs after implantation of the embryo during the process of gastrulation. Signaling proteins belonging to the BMP and WNT families are key gastrulation factors that mediate induction of the primitive streak in the embryo and can induce primitive streak derivatives in human ESCs (hESCs) and mouse ESCs (mESCs) (Bakre et al., 2007; Blauwkamp et al., 2012; Davidson et al., 2012; Drukker et al., 2012; Gadue et al., 2006; Lako et al., 2001; Lindsley et al., 2006; Nostro et al., 2008; Sumi et al., 2008; ten Berge et al., 2008). However, BMP4 additionally induces trophoblast (Drukker et al., 2012; Xu et al., 2002), complicating efforts to obtain single lineages. Furthermore, other reports show that both BMP and WNT signals support the self-renewal of mESCs instead (Hao et al., 2006; Ogawa et al., 2006; Singla et al., 2006; ten Berge et al., 2011; Ying et al., 2003). These conflicting reports may reflect the action of BMP and WNT signals on different pluripotent states, as the epiblast of post implantation mouse embryos can also give rise to a pluripotent cell type, the epiblast stem cell (EpiSC) (Brons et al., 2007; Tesar et al., 2007). EpiSCs are developmentally more advanced than mESCs and possess different morphology, growth factor requirements, gene expression profile, and epigenetic state (Brons et al., 2007; Tesar et al., 2007). They can generate teratomas, a measure of pluripotency, but unlike mESCs are not competent to contribute to blastocyst chimeras.

EpiSCs express many differentiation factors present in the primitive streak (Brons et al., 2007; Tesar et al., 2007) and were found to comprise heterogeneous populations of cells with distinct potency (Bernemann et al., 2011; Tsakiridis et al., 2014). This suggests that EpiSCs are to some extent prespecified, and their pluripotent state has therefore been designated "primed," as opposed to the unspecified "naïve" pluripotent state of mESCs (Nichols and Smith, 2009). Similar observations were made for hESCs, consistent with them occupying a primed pluripotent state (Blauwkamp et al., 2012; Davidson et al., 2012; Drukker et al., 2012; Stewart et al., 2006). Interestingly, for both EpiSCs and hESCs, it has been shown that endogenous WNT proteins, produced by the cells themselves, drive prespecification of the cells (Blauwkamp et al., 2012; Frank et al., 2012; Sumi et al., 2013; Tsakiridis et al., 2014).

Here we address the consequences of endogenous WNT signals for directed differentiation and self-renewal of human and mouse pluripotent cells. We show that

endogenous WNT signals mediate differentiation decisions in response to BMP signals and furthermore that they are the main cause of spontaneous differentiation in both hESCs and EpiSCs.

RESULTS

BMP4-Induced Differentiation of EpiSCs Is Mediated by WNT Signals

Both WNT and BMP signals are implicated in the initiation of gastrulation and induction of the primitive streak. To monitor these processes in vitro, we established EpiSCs carrying the T-GFP reporter for the primitive streak marker *Brachyury* by differentiating T-GFP ESCs (Fehling et al., 2003) into EpiSCs by culture in FGF2 and ACTIVIN. We included IWP2, a small molecule inhibitor that blocks the biosynthesis of mature WNT proteins (Chen et al., 2009), to increase the efficiency of differentiation (ten Berge et al., 2011). Phenotypic and functional assays verified the complete differentiation (Figures S1A–S1D available online).

Treatment of the T-GFP EpiSCs with either WNT3A or BMP4, in the presence of ACTIVIN and FGF2, strongly induced reporter expression, followed by loss of the pluripotency marker SSEA1 (Figure 1A). However, in the BMP4-treated cells, these events were delayed, possibly because BMP4 may act indirectly, by inducing WNT signals in EpiSCs (Figure 1A). Indeed, BMP4 protein strongly induced a reporter for WNT signaling in Axin2-LacZ EpiSCs (ten Berge et al., 2011) (Figure 1B). This was due to the induction of endogenous WNT proteins as reporter expression was inhibited by IWP2 (Figure 1B). Importantly, IWP2 prevented not only the induction of T-GFP but also the loss of SSEA1 in response to BMP4 (Figure 1A), suggesting that BMP4-mediated exit from pluripotency requires the activation of WNT. Indeed, while both WNT3A and BMP4 induced expression of differentiation markers and loss of EpiSC markers, IWP2 prevented the gain or loss of these markers in response to BMP4, demonstrating that it relied on the induction of WNT signals (Figures 1C and S1E). IWP2 did not interfere with WNT signal transduction or differentiation per se since it did not block the effects of WNT3A (Figure S1F).

We used RNA-Seq to analyze the interactions between BMP4 and WNT in EpiSCs treated for 48 hr in the presence of ACTIVIN and FGF2. Principal component analysis showed that the BMP4- and/or WNT3A-treated samples separated from all other samples along the first component, whereas the IWP2-treated samples clustered together, regardless of the presence of BMP4 (Figure 1D). Interestingly, the WNT3A-treated samples clustered together with the BMP4-treated sample and induced the same mesodermal markers, such as *Kdr*, *Mesp1*, and *Tbx6* (Figures 1D and 1E). BMP4 was unable to induce these markers in the presence of IWP2 despite inducing the canonical BMP target *Id1*, showing that IWP2 did not interfere with BMP signal transduction (Figure 1E). These data show that the gene-expression changes induced by BMP4 in EpiSCs are to a large extent secondary to activation of WNT proteins.

Feedback loops between signaling factors are an important element of gastrulation (Ben-Haim et al., 2006; Tortelote et al., 2013). We therefore analyzed the short-term (2–6 hr) induction of the gastrulation factors *Nodal*, *Wnt3*, and *Fgf8* by BMP4 and/or WNT3A. While BMP4 induced *Wnt3*, WNT3A induced all three factors, and the highest induction of *Wnt3* was obtained using both signals (Figure 1F). These observations explain why BMP signals are not required for primitive streak induction once WNT signals have been activated. No induction of the WNT target *Axin2* by BMP4 or the BMP-target *Id1* by WNT3A was observed within the 6 hr timeframe (Figure 1F). However, *Id1* is somewhat induced in the 48 hr WNT3A-only condition, suggesting that the differentiating cells activate endogenous BMP signals (Figure 1E). Nonetheless, T-GFP induction was not suppressed by the BMP inhibitor LDN193189, indicating that it did not require BMP signals (Figure 1A). Finally, IWP2 prevented the loss of both OCT4- and SOX2-positive as well as SSEA1-positive EpiSCs in response to BMP4 (Figures 1G and S1G). Combined, these data indicate that induction of EpiSC differentiation by BMP4 is mediated by the induction of WNT signals.

Endogenous WNT Proteins Induce Differentiation and Loss of Pluripotency in EpiSCs

In the course of our studies, we found that T-GFP EpiSCs spontaneously induced a significant GFP-positive population (Figure 1A, +vehicle). This induction was suppressed either by IWP2 or by the WNT antagonist FZ8CRD, a soluble domain of the WNT receptor that binds and sequesters WNT proteins, indicating that it was due to endogenous WNT proteins (Figure 1A). The presence of endogenous WNT activity was further confirmed by the spontaneous LACZ activity evident in Axin2-LacZ EpiSCs, which was also suppressed by IWP2 (Figure 1B). Moreover, multiple *Wnt* genes were expressed in EpiSCs, in particular *Wnt3* (Figure S2A). These observations are in line with a recent report showing that endogenous WNT signals specify a fraction of EpiSCs toward primitive-streak lineages (Tsakiridis et al., 2014). Clonal assays showed that these specified cells were not committed to differentiation and maintained a pluripotent phenotype (Tsakiridis et al., 2014).

However, we noticed that the GFP-positive cells showed a shift to lower SSEA1 expression, suggesting that some of them lost pluripotency (Figure 1A). We therefore sorted the cells based on T-GFP intensity and assessed their potential to establish colonies or to form embryoid bodies (EBs), both measures of pluripotency. A clear negative correlation

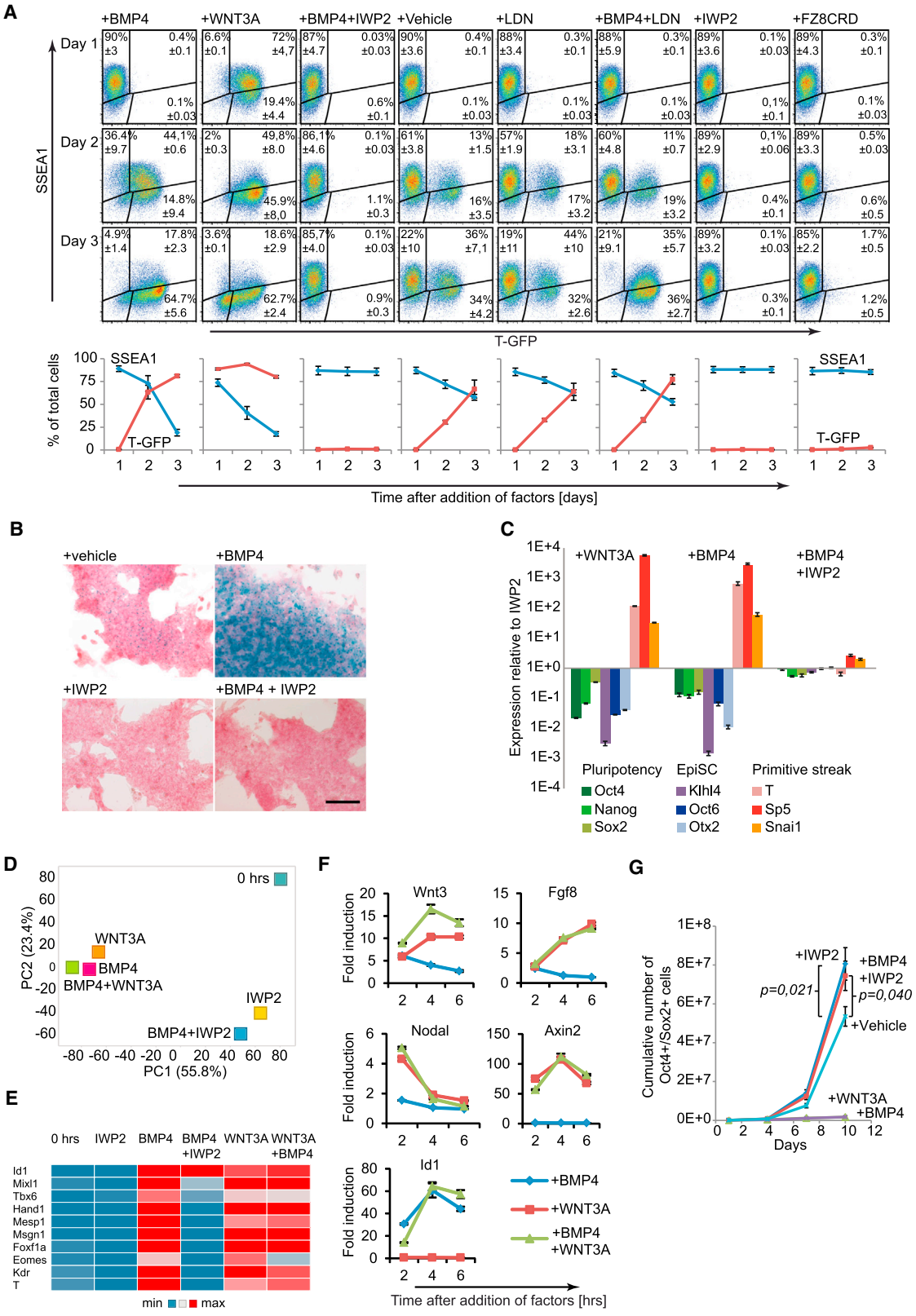

(legend on next page)

was visible between the level of GFP and potential to establish NANOG-positive colonies (Figures 2A, S2B, and S2C). Likewise, cells with higher levels of GFP produced smaller EBs, while the cells with the highest level failed to form EBs at all (Figures 2B and S2D). Moreover, these cells downregulated SOX2 and OCT4 (Figure 2B). These data show that the T-GFP-positive population is enriched for cells that have lost pluripotency.

We next tested whether WNT inhibition would prevent this loss of pluripotency. When analyzed for SSEA1, multiple EpiSC lines all displayed substantial levels of SSEA1-negative cells, indicating significant differentiation (Figures 2C and S2E, vehicle). However, in the presence of IWP2, more than 90% of the cells expressed SSEA1 (Figures 2C and S2E). In addition, RT-PCR and immunostaining showed that IWP2 not only repressed primitive streak markers but also raised the level of the pluripotency markers *Oct4*, *Nanog*, and *Sox2* (Figures 2D and S1E). Moreover, IWP2 substantially enhanced the expansion of OCT4- and SOX2-positive or SSEA1-positive cells (Figures 1G and S1G). In line with a recent report (Sumi et al., 2013), suppression of endogenous WNT signals also greatly enhanced the derivation of novel EpiSC lines from 25% (four lines from 16 E5.5 embryos) to 79% (15 of 19). These data show that endogenous WNT signals induce loss of pluripotency in a subset of EpiSCs, and WNT inhibition suppresses this spontaneous differentiation, greatly enhancing their self-renewal and derivation efficiency. In fact, certain cell lines, e.g., the T-GFP EpiSCs, could essentially not be maintained in the absence of IWP2 as they progressively accumulated differentiated cells (Figure 1A, +vehicle).

To identify the differentiation pathways induced by endogenous WNT signals we compared the transcriptomes of EpiSCs maintained in the presence or absence of IWP2. Most differences were due to a set of genes that was repressed by IWP2 (Figure 2E), with 321 genes downregulated and 87 genes upregulated in response to IWP2 (Table S1). Using gene set enrichment analysis (Subramanian et al., 2005), we found that a set of 29 genes first expressed around the start of gastrulation (Pfister et al., 2007) was strongly enriched in conventional EpiSCs when compared with EpiSCs treated with IWP2 (Figure 2F; Table S2). We next looked for signatures of more committed cell types that derive from the primitive streak. A set of 98 genes expressed in committed human- and mouse-definitive endoderm and endoderm precursors (Hou et al., 2007; McLean et al., 2007; Ogaki et al., 2011; Tada et al., 2005) was highly enriched in conventional EpiSCs (Figure 2F; Table S3). Since some of these genes are also expressed in mesoderm progenitors, we created a gene set consisting of 154 genes specifically expressed in E7.5 endoderm versus mesoderm and ectoderm (Gu et al., 2004) and found strong enrichment of this set in conventional EpiSCs (Figure 2F; Table S4). Furthermore, a panel of genes associated with the committed endoderm state showed consistent repression in response to IWP2 (Figure 2G). In contrast, a set of 155 genes expressed in E7.5 mesoderm and ectoderm versus endoderm (Gu et al., 2004) showed no enrichment (Figure 2F; Table S5) and committed mesoderm markers such as *Mesp1*, *Meox1*, *Kdr*, *Hand1*, *Msgn1*, *Foxf1a*, *Tlx2*, or *Tbx6* ranked low in the comparison (Table S5). Anterior neurectoderm genes did not increase in response to IWP2 (Figure S2F), indicating that endogenous WNT signals were not required to inhibit neural differentiation. These findings show that endogenous WNT signals induce a committed definitive endoderm state in a subset of EpiSCs, explaining the loss of pluripotency in response to endogenous WNT signals.

WNT Inhibition Maintains EpiSCs in a Pregastrula Epiblast Stage

Despite their origin from the pregastrula epiblast, transcriptome comparisons indicate that EpiSCs are more similar to the late-gastrula-stage epiblast (Kojima et al., 2014). To test whether WNT inhibition maintains EpiSCs in a state closer to that of the pregastrula epiblast, we compared their transcriptomes with those of epiblasts derived from embryos ranging from the cavity (Cav) stage to the prestreak (PS),

Figure 1. BMP4-Induced Differentiation of EpiSCs Depends on WNT Signals

(A) Flow cytometry plots of T-GFP EpiSCs treated with the indicated factors and analyzed for T-GFP and SSEA1. The cells were maintained in the presence of IWP2 prior to the experiment. Line plots indicate the mean of three independent experiments ± SEM.

(B) Axin2-LacZ EpiSCs treated for 3 days with the indicated factors and stained for LACZ (blue).

(C) RT-PCR gene expression profiles of GFP9 EpiSCs treated for 2 days with the indicated factors, plotted relative to EpiSCs maintained in the presence of IWP2 (n = 3, mean ± SEM).

(D) Principal component analysis of transcriptomes of GFP9 EpiSCs treated for 48 hr with the indicated factors or untreated (0 hr). The percentage of variance explained by the principal components is indicated between parentheses.

(E) Heat map of selected gene expression levels in GFP9 EpiSCs treated for 48 hr with the indicated factors, determined by RNA-Seq.

(F) Time course RT-PCR analysis of indicated genes in GFP9 EpiSCs following treatment with the indicated factors (n = 3, mean ± SEM).

(G) Plot showing the expansion of OCT4- and SOX2-positive 129S2C1a EpiSCs in the indicated conditions (three independent experiments, mean ± SEM).

The scale bar represents 200 μm. See also Figure S1.

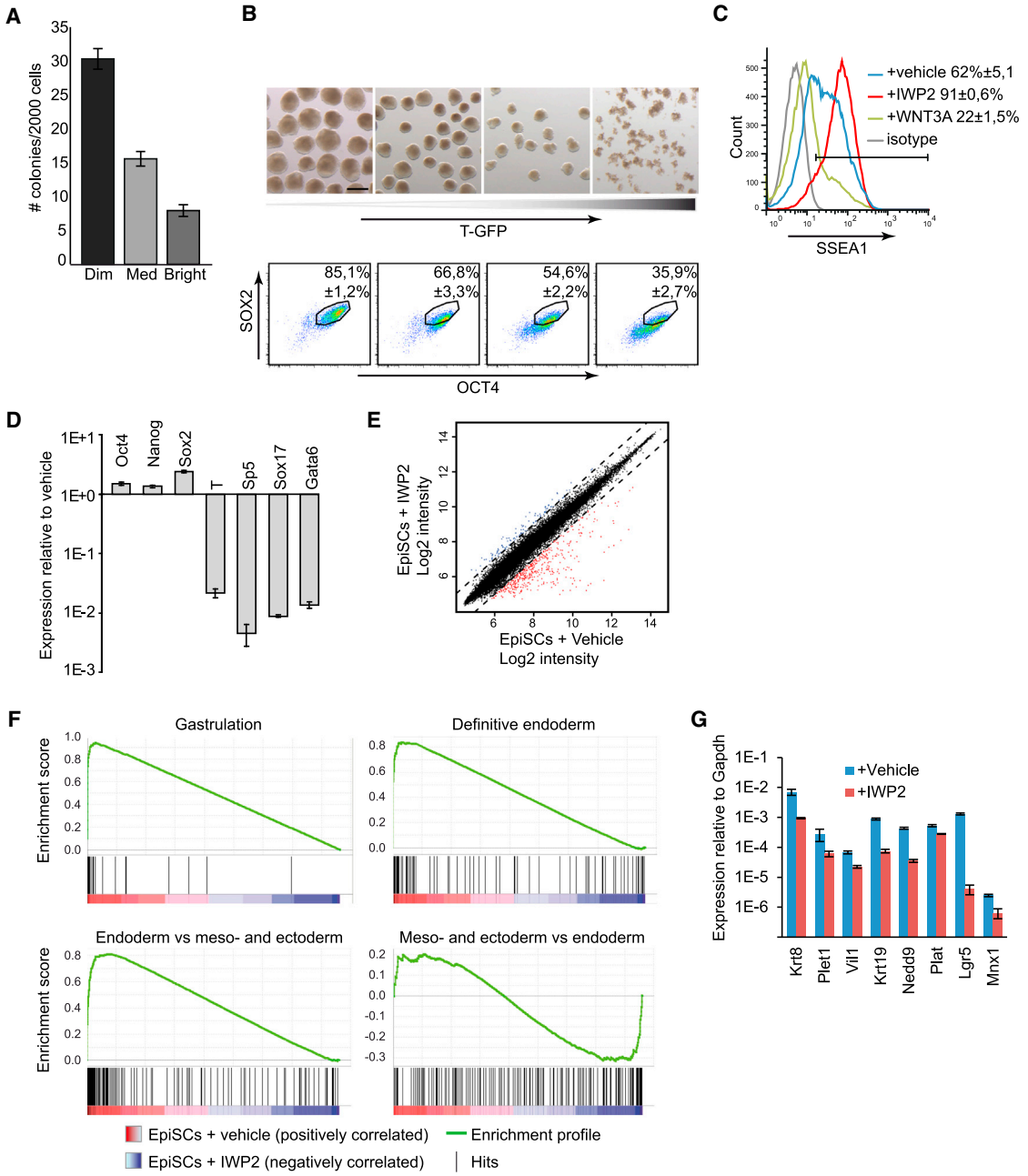

Figure 2. Endogenous WNT Proteins Induce Loss of Pluripotency in EpiSCs

(A) T-GFP EpiSCs were sorted into three categories based on GFP and assayed for their ability to establish NANOG-positive colonies (three independent experiments, mean ± SEM).

(B) T-GFP EpiSCs were sorted into four categories based on GFP and assayed for their ability to establish EBs (top) or analyzed by flow cytometry for SOX2 and OCT4 (bottom, three independent experiments, mean ± SEM).

(C) Flow cytometry histogram showing T-GFP EpiSCs treated for 3 days with the indicated factors and analyzed for SSEA1 (three independent experiments, mean ± SEM).

(D) Real-time RT-PCR gene expression profiles of 129S2C1a EpiSCs cells treated for 3 days with IWP2, plotted relative to untreated EpiSCs (three independent experiments, mean ± SEM).

(E) Scatter plot comparing the global gene expression levels of GFP9 EpiSCs cultured in the presence or absence of IWP2. The dotted lines delineate the boundaries of 2-fold difference in gene expression levels. Genes expressed more than 2-fold higher or lower in the presence of IWP2 are plotted in blue or red, respectively.

(legend continued on next page)

late mid streak (LMS), late streak (LS), no bud (OB), early bud (EAB), and late bud (LB) stage, obtained using Illumina bead-chip arrays (Kojima et al., 2014). A normalization procedure matched the distribution of the expression values from our Affymetrix to the Illumina platform, and the genes that were at least 1.5-fold differentially expressed in response to IWP2 (1,066 gene identifications shared between both platforms) were analyzed using principal component analysis. As observed before (Kojima et al., 2014), the first component separated the embryo-derived samples from the EpiSCs, whereas the second component separated the embryo-derived samples according to their developmental stage (Figure 3A). Importantly, while the regular EpiSCs aligned at the early bud stage, EpiSCs maintained in the presence of IWP2 aligned between the prestreak and early-streak stages, showing that their transcriptome is indeed more similar to that of the pregastrula epiblast (Figure 3A).

We tested the pregastrula state of EpiSCs maintained with IWP2 using two functional assays. First, a small percentage of EpiSCs can revert to the ESC state when transferred to ESC conditions (Greber et al., 2010), and we found that IWP2 treatment strongly raised this reversal efficiency (Figure 3B). This indicates that IWP2 caused many more cells to occupy a state of pluripotency sufficiently close to that of ESCs to make the transition. Second, in contrast to epiblast from the gastrula, the pregastrula epiblast can contribute to chimeras upon blastocyst injection (Gardner et al., 1985). However, EpiSCs rarely contribute to blastocyst chimeras but rather, corresponding to their late-gastrula stage character, can integrate when introduced into the primitive streak (Huang et al., 2012; Kojima et al., 2014). We derived EpiSCs from E6.5 transgenic embryos carrying either a Rosa26-LacZ or Actin-GFP reporter in the presence of IWP2, cultured the cells for five passages, and performed blastocyst injections. We obtained 3 chimeras out of 14 E10.5 embryos from the Rosa26-LacZ EpiSCs, and 1 chimera out of 14 embryos from the Actin-GFP-derived EpiSC line GFP9 (Figure 3C). X-gal and immunostainings demonstrated integration into multiple tissues, including the neural tube, somite, nephrogenic cord, body wall, splanchnopleure, and parts of the gut tube (Figure S3A). Together, these tests strongly support the pregastrula character of EpiSCs shielded from WNT signals. Moreover, they indicate that the ability to contribute to blastocyst chimeras does not distinguish naive from primed pluripotent cells.

We considered several explanations for the blastocyst compatibility of IWP2-treated EpiSCs. First, some cells may be reprogrammed to the naive state. However, IWP2 induced no increase in *Tbx3*, *Dppa3*, *Zfp42*, *Klf4*, *Dppa5*, or other naive markers (Figure 3D; Table S1). Second, IWP2 may stabilize a minor fraction of EpiSCs that contributes to blastocyst chimeras, marked by the Oct4-GFP reporter GOF18 (Han et al., 2010). IWP2 did however not enhance the GFP-positive fraction and sorted GFP-positive cells lost GFP expression regardless of the presence of IWP2 (Figures S3B and S3C). Third, E-CADHERIN overexpression allows EpiSCs to participate in blastocyst chimeras (Ohtsuka et al., 2012). We observed higher *E-cadherin* expression and strong E-CADHERIN staining throughout the cultures in the presence of IWP2, similar in strength as in ESCs, whereas staining was faint and patchy in regular EpiSCs (Figures 3E and 3F). Furthermore, WNT3A induced the *E-cadherin* repressor *Snai1* and *N-cadherin* and downregulated *E-cadherin* in EpiSCs (Figure 3G). These observations indicate that endogenous WNT proteins repress *E-cadherin* in EpiSCs, thereby reducing their ability to integrate in the pregastrulation epiblast.

WNT inhibition repressed multiple differentiation genes, including *Eomes*, *Foxa2*, *Gata6*, *Lefty2*, and *Sox17*, to the same level as in ESCs, indicating that they are not EpiSC markers (Figure 3D). We screened our gene expression data for potential markers for genuine EpiSCs, maintained in the presence of WNT inhibition (Figure 3H), and identified CD38, CD107/KIT, CD105/ENDOGLIN, and CD44 as cell surface markers suitable to separate ESCs and EpiSCs by flow cytometry (Figure 3I) and OCT6 as a nuclear marker for genuine EpiSCs (Figure 3J).

Next, we addressed whether the differentiation-inducing effect of WNT on EpiSCs explains the conflicting reports on the role of WNT in ESCs. While we previously demonstrated that endogenous WNT signals support ESC self-renewal by inhibiting their differentiation into EpiSCs (ten Berge et al., 2011), we and others also demonstrated that WNT signals induce differentiation of ESCs in EBs (Nostro et al., 2008; ten Berge et al., 2008). However, a transient EpiSC signature has been detected in differentiating EBs (Zhang et al., 2010). This could be the result of a shutdown of the WNT pathway in EBs, which would induce differentiation of ESCs into EpiSCs. When we generated EBs from ESCs carrying the 7xTcf-GFP reporter for WNT signaling (ten Berge et al., 2008), we observed rapid downregulation of the WNT reporter, followed by loss of the ESC

(F) Gene set enrichment analysis plots demonstrating the enrichment of the indicated gene sets in EpiSCs cultured in the absence versus the presence of IWP2.

(G) RT-PCR analysis for definitive endoderm genes in EpiSCs, in response to IWP2 (three biological replicates using 129S2C1a, Axin2LacZ, and GFP9 EpiSCs, mean ± SEM).

Scale bar represents 200 μm. See also Figure S2.

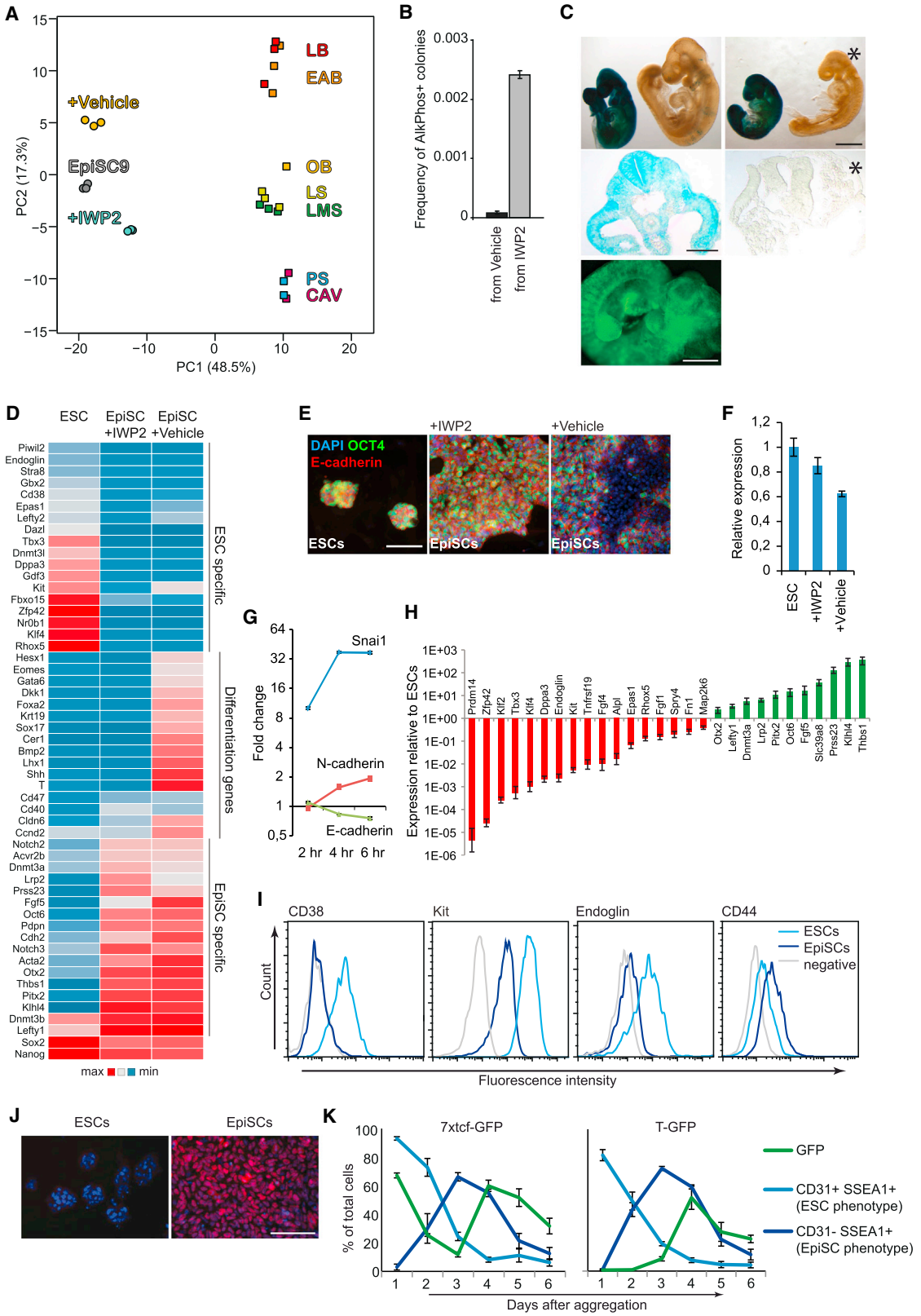

(legend on next page)

marker CD31 (Figure 3K). However, the cells maintained expression of the pluripotency marker SSEA1, suggesting they converted into EpiSCs. Following this transition, the WNT reporter was induced while SSEA1 was lost (Figure 3K), suggesting that endogenous WNTs now acted as differentiation signals. Indeed, using T-GFP ESCs, we observed induction of the differentiation reporter following the transition of the ESCs into EpiSCs (Figure 3K). Thus, EBs first mediate the conversion of ESCs into EpiSCs; only then are endogenous WNT signals activated that induce their differentiation.

Inhibition of Endogenous WNT Signals Prevents the Accumulation of Differentiated Cells in hESC Cultures

It is thought that hESCs occupy a state of primed pluripotency like that of mouse EpiSCs, rather than the naive pluripotency of mESCs (Nichols and Smith, 2009). hESC cultures experience substantial spontaneous differentiation and require frequent manual removal of accumulations of differentiated cells. We investigated whether commitment to differentiation could be prevented by inhibition of endogenous WNT signals, similar to what we showed for EpiSCs.

In the presence of IWP2 or FZ8CRD, both H1 and H9 hESCs established flatter, sharper edged colonies with very little evidence of differentiated cells, whether cultured on mouse embryo fibroblasts (MEFs) or in mTESR1, a serum- and feeder-free medium (Figures 4A and S4A). When cultured in standard conditions, both H1 and H9 hESCs formed patches of BRACHYURY- and GATA4-positive cells (Figures S4B and S4C), and significant proportions of the cells lacked NANOG, OCT4, or SOX2 (Figures 4B and S4D). In contrast, no BRACHYURY or GATA4 was visible when the cells were cultured in the presence of IWP2 (Figures S4B and S4C), and the proportion of cells lacking the pluripotency factors was strongly reduced (Figures 4B and S4D). A recently introduced defined medium, E8, performed better yet IWP2 significantly improved the proportion of cells expressing the pluripotency factors (Figure 4B). RT-PCR analysis confirmed that IWP2 repressed multiple markers of mesendodermal differentiation and enhanced expression of pluripotency markers, while neurectodermal markers either showed minor changes or were downregulated (Figures 4C and S4E). These data suggest that WNT inhibition prevents the spontaneous mesendodermal differentiation of hESCs, while not increasing neurectodermal differentiation.

We next tested whether WNT inhibition obviated the need for manual removal of differentiated cells during routine culture of hESCs. With manual cleaning, both H1 and H9 hESCs maintained persistent populations of cells lacking one or more of the pluripotency factors, while in the absence of cleaning this population progressively increased (Figures 4D, S4F, and S4H). Strikingly, IWP2 maintained pluripotency factor expression in most cells in the absence of cleaning (Figures 4D, S4F, and S4H). Furthermore, IWP2 prevented the accumulation of cells expressing the hESC differentiation marker SSEA1, which otherwise rapidly accumulated (Figures 4E, S4G, and S4H). Finally, both H1 and H9 cells cultured for 10 passages in IWP2 efficiently formed teratomas, indicating that they retained their pluripotency (Figure S4I). Combined, these

Figure 3. WNT Inhibition Maintains EpiSCs in a Pregastrula Epiblast Stage

(A) Transcriptomes from primary epiblasts dissected from embryos ranging from cavity to late bud stages and from the EpiSC line EpiSC9 were obtained from GEO (GSE46227) and combined with six microarray gene expression data sets from GFP9 EpiSCs cultured with and without IWP2 and analyzed by principal component analysis. The percentage of variance explained by the principal components is indicated between parentheses.

(B) Reversal efficiency of T-GFP EpiSCs. Prior to start of the reversal experiment, the cells were maintained in the presence or absence of IWP2 as indicated (n = 3, mean ± SEM).

(C) (Upper) X-gal stained chimeras derived from blastocyst injections of passage 5 Rosa26-LacZ EpiSCs. (Middle) Sections to indicate EpiSC contribution (blue). Asterisk indicates a nonchimeric littermate. (Lower) Chimera derived from blastocyst injections of passage 5 GFP9 EpiSCs. Green fluorescence indicates EpiSC contribution.

(D) Heat map of selected gene expression levels of ESCs and GFP9 EpiSCs cultured in the presence or absence of IWP2 and analyzed by microarray.

(E) E-CADHERIN and OCT4 immunofluorescence images of EpiSCs and ESCs.

(F) RT-PCR for *E-cadherin* in EpiSCs and ESCs (three biological replicates using 129S2C1a, Axin2LacZ, and GFP9 EpiSCs, mean ± SEM).

(G) Time course RT-PCR analysis of indicated genes in GFP9 EpiSCs following treatment with WNT3A (n = 3, mean ± SEM).

(H) Real-time RT-PCR gene expression analysis of FVB EpiSCs relative to ESCs for a range of genes found by microarray to be differentially expressed between EpiSCs and ESCs (n = 3, mean ± SEM).

(I) Flow cytometry histograms showing surface markers distinguishing ESCs (CD38, KIT, and ENDOGLIN) and EpiSCs (CD44).

(J) OCT6 immunostaining (red) of 129S2C1a EpiSCs and ESCs (blue, DAPI).

(K) The indicated ESC lines were aggregated into EBs and analyzed daily by flow cytometry for expression of reporter and the indicated cell surface markers (three independent experiments, mean ± SEM).

Scale bar represents 1 mm (C, embryos), 200 μm (C, section), 100 μm (E and J). See also Figure S3.

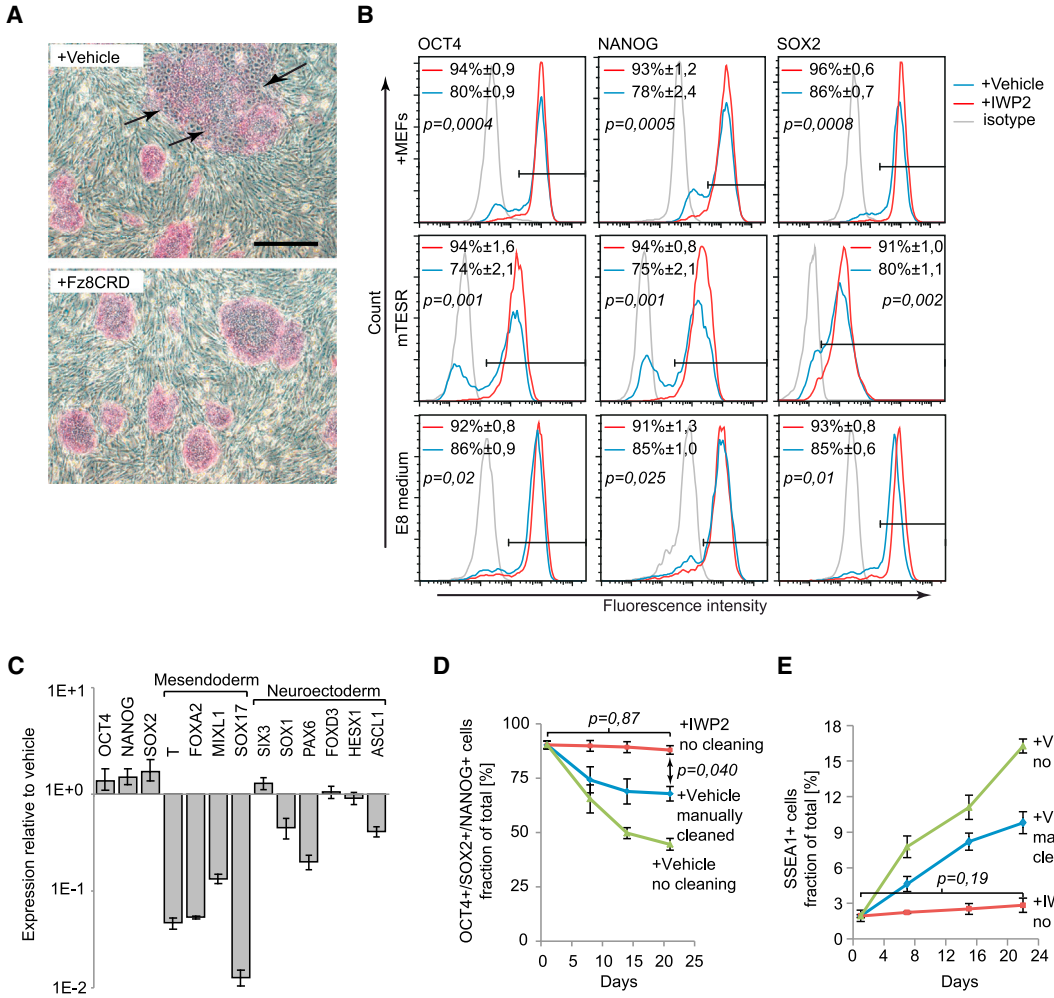

Figure 4. Inhibition of Endogenous WNT Signals Prevents Accumulation of Differentiated Cells in hESC Cultures

(A) H1 hESCs cultured for 5 days at the indicated conditions and stained for alkaline phosphatase (red). Arrows indicate differentiating areas of the colonies.

(B) Flow cytometry histograms showing H1 hESCs cultured for 7 days in the presence or absence of IWP2 and analyzed for NANOG, OCT4, and SOX2 (three independent experiments, mean ± SEM).

(C) Real-time RT-PCR gene expression profiles of H1 hESCs cultured for 6 days in the presence of IWP2, plotted relative to untreated cells (n = 3, mean ± SEM).

(D) Percentage of H1 hESCs triple positive for NANOG, OCT4, and SOX2 in the indicated conditions and procedures (three independent experiments, mean ± SEM).

(E) Percentage of H1 hESCs expressing SSEA1 in the indicated conditions and procedures (three independent experiments, mean ± SEM). Scale bar represents 500 μm. See also Figure S4.

data show that inhibition of endogenous WNT signals prevents the accumulation of differentiated cells in hESC cultures and obviates the need for their manual removal.

BMP4 Induces Both WNT-Dependent and WNT-Independent Differentiation Pathways in hESCs

We next investigated whether WNT signals mediate BMP-induced differentiation in hESCs. Similar to the observations with mouse EpiSCs, both WNT3A and BMP4 protein induced BRACHYURY and GATA4 in H1 hESCs, with concomitant loss of OCT4 (Figure S5A). Flow cytometry indicated a strong induction of the mesoderm marker ROR2 (Drukker et al., 2012), together with suppression of pluripotency factors (Figures 5A, S5B, and S5C). RT-PCR analysis showed induction of additional primitive streak and mesoderm markers (Figure 5B). Furthermore, induction of *WNT3* in response to BMP4 suggested that in hESCs too mesodermal induction was mediated by

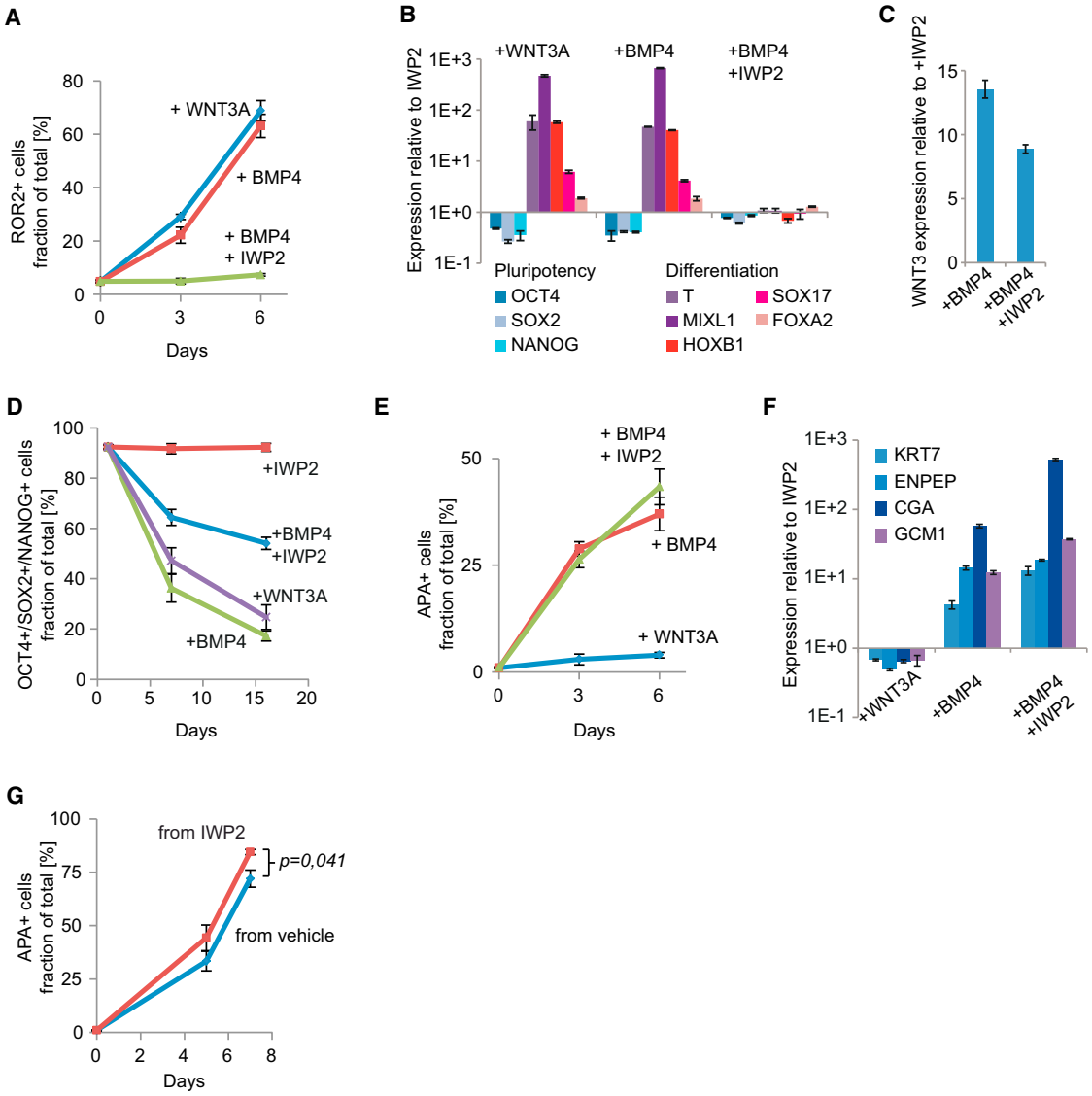

Figure 5. BMP4 Induces Both WNT-Dependent and WNT-Independent Differentiation Pathways in hESCs

(A) H1 hESCs were cultured with the indicated factors for 3 or 6 days and analyzed by flow cytometry for the mesodermal marker ROR2 (three independent experiments, mean ± SEM).

(B) Real-time RT-PCR gene expression profiles of H1 hESCs cultured for 3 days in the indicated factors, plotted relative to cells maintained in the presence of IWP2 (n = 3, mean ± SEM).

(C) *WNT3* expression level 6 hr after induction of H1 hESCs with the indicated factors, plotted relative to cells maintained in IWP2 (n = 3, mean ± SEM).

(D) H1 hESCs cultured in the presence of the indicated factors and analyzed at several time points by flow cytometry for NANOG, OCT4, and SOX2. Plotted is the percentage of cells positive for all three markers (three independent experiments, mean ± SEM).

(E) H1 hESCs cultured with the indicated factors for 3 or 6 days and analyzed by flow cytometry for the trophoblast marker APA (three independent experiments, mean ± SEM).

(F) Real-time RT-PCR gene expression profiles of H1 hESCs cultured for 4 days in the indicated factors, plotted relative to cells maintained in the presence of IWP2 (n = 3, mean ± SEM).

(G) H1 hESCs maintained in the presence or absence of IWP2 prior to the experiment were differentiated with BMP4 in the presence of IWP2 and analyzed by flow cytometry for the trophoblast marker APA (three independent experiments, mean ± SEM).

See also Figure S5.

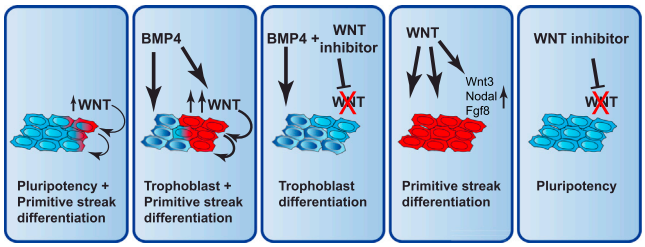

Figure 6. BMP and Endogenous WNT Signals Act Sequentially to Induce Shared and Distinct Differentiation Pathways in hESCs

(Left to right) Endogenous WNT proteins induce differentiation toward primitive streak lineages (red), reducing self-renewal. BMP4 induces both trophoblast (dark blue) and, mediated by endogenous WNTs, primitive streak lineages. In the presence of WNT inhibitors, BMP4 induces only trophoblast and no primitive streak lineages. WNT signals upregulate gastrulation factors and induce primitive streak lineages. WNT inhibitors block spontaneous differentiation, obviating the need to remove differentiated cells during culture.

endogenous WNT (Figure 5C). Indeed, IWP2 prevented mesodermal induction in response to BMP4 (Figures 5A, 5B, and S5A). IWP2 did not abolish the induction of *WNT3*, indicating that it did not directly interfere with BMP4 signaling (Figure 5C). Importantly, IWP2 reduced but did not prevent the loss of the pluripotency markers in response to BMP4 (Figures 5D and S5C). These data show that BMP4 induces mesodermal lineages in hESCs indirectly, via induction of WNT proteins, but also suggest that it induces an alternative differentiation pathway that is WNT independent.

In addition to mesodermal lineages, hESCs have the ability to differentiate into trophoblast (Pera et al., 2004; Xu et al., 2002), and it has recently been shown that a mixture of mesoderm- and trophoblast-committed cells emerge in response to BMP4 (Drukker et al., 2012). In agreement with this study, both flow cytometry for the trophoblast surface marker APA (Drukker et al., 2012), and RT-PCR for the trophoblast markers *KRT7*, *ENPEP*, *CGA*, and *GCM1* show that BMP4 induces the emergence of trophoblast progenitors (Figures 5E, 5F, and S5D). Importantly, WNT3A did not induce trophoblast differentiation, nor was the induction of the trophoblast markers by BMP4 inhibited by IWP2 (Figures 5E and 5F). Combined, these data show that BMP4 can induce the emergence of trophoblast-committed cells from hESCs in a WNT-independent manner, whereas the induction of mesoderm-committed cells requires the action of WNT proteins, either induced endogenously by BMP4 or added directly to the cells.

Finally, a reasonable assumption would be that hESCs maintained in the presence of IWP2 are better substrates for differentiation as they contribute fewer undesired lineages to the population. Indeed, when differentiated toward trophoblast by BMP4+IWP2, H1 hESCs that were maintained in the presence of IWP2 produced more APA+ cells than regular H1 cells (Figures 5G and S5E).

DISCUSSION

This work shows that endogenous WNT signals are major hidden factors in the differentiation of hESCs and EpiSCs and affect the outcome of directed differentiation protocols in hitherto unappreciated ways. We show that WNT signals induce the main gastrulation factors *Nodal*, *Wnt3*, and *Fgf8* and are required and sufficient for the induction of mesoderm by the commonly used mesoderm inducer BMP4. A surprising finding is that BMP4 induces both mesoderm as well as trophoblast-committed cells from hESCs, but only mesoderm induction requires the activation of *WNT* genes by BMP4.

We further show that endogenous WNT signals interfere with self-renewal of hESCs and mEpiSCs. Endogenous WNTs push the aggregate developmental phenotype of EpiSCs to that reminiscent of late-gastrula stage epiblast, consisting of a mixture of genuine EpiSCs with cells in various stages of differentiation, including cells committed to the definitive endoderm lineage. WNT inhibition prevents the induction of differentiation genes and commitment to endoderm, thereby maintaining a high percentage of genuine EpiSCs displaying their pregastrula phenotype, as evidenced by their contribution to blastocyst chimeras. A similar process takes place in hESCs, where we show that WNT inhibition is so effective in suppressing differentiation that it obviates the need for manual removal of differentiated cells during routine culture.

These findings are summarized in Figure 6, and they have obvious ramifications for the guided differentiation of hESCs. For instance, to induce trophoblast one should stimulate with BMP4 in the presence of a WNT inhibitor to avoid induction of mesoderm. Conversely, mesoderm is best obtained using WNT3A in lieu of BMP4 to avoid trophoblast induction. Furthermore, WNT-inhibited hESCs differentiate more efficiently to the trophoblast lineage, suggesting that genuine EpiSCs and hESCs, maintained as homogeneous undifferentiated populations by WNT inhibition, are superior substrates for differentiation as they contribute fewer undesired lineages to the population. We also find that different cell lines and culture media display various tendencies for endogenous WNT-induced differentiation, affecting their suitability for specific purposes such as mesoderm or neural differentiation. This may also influence to what extent WNT inhibition supports their self-renewal or improves their subsequent differentiation. Another interesting observation is that spontaneous endogenous WNT signals induce endoderm

in EpiSCs, consistent with the finding that low levels of WNT3A (25 ng/ml) induce definitive endoderm (D'Amour et al., 2006), whereas high levels of WNT3A (250 ng/ml) induce mesoderm. This may reflect a later function for WNT in redirecting primitive streak-specified cells from endoderm to mesoderm (Loh et al., 2014). Finally, ESCs are commonly aggregated into EBs for the derivation of mesendodermal lineages. We now show that EBs mediate the transition of mESCs into EpiSCs, which is followed by activation of an endogenous WNT gradient and primitive streak induction (ten Berge et al., 2008). A more controlled way of inducing mesendodermal lineages would be by directly inducing genuine EpiSCs with defined levels of WNT signals.

The sequential action of BMP and WNT signals that we uncover here is consistent with embryological findings: *Bmp4* is expressed prior to gastrulation in the extraembryonic ectoderm (Waldrip et al., 1998), both *Wnt3* and active beta-catenin have been detected in the prestreak epiblast bordering this *Bmp4*-expressing region (Mohamed et al., 2004; Rivera-Pérez and Magnuson, 2005), and WNT pathway activation in the epiblast is required for primitive streak induction (Haegel et al., 1995; Huelsken et al., 2000; Liu et al., 1999). The spatiotemporal expression patterns of *Bmp4* and *Wnt3* are therefore consistent with a role for BMP4 in inducing *Wnt3* in the primitive streak-forming region. This is supported by the observations that BMP4 induces *Wnt3* expression in epiblast explants (Ben-Haim et al., 2006), and *Bmp4* loss of function mutants fail to initiate gastrulation (Winnier et al., 1995). Since we find that WNT signals induce the essential gastrulation factors *Wnt3*, *Nodal*, and *Fgf8* in the epiblast, this suggests that, upon WNT3 induction, the primitive streak can continue to expand distally because of continuous induction of the gastrulation factors, including WNT3 itself, by WNT3.

A recent study shows that a subpopulation of EpiSCs expressing a transgenic *Brachyury* reporter displays reversible primitive streak characteristics, i.e., while biased toward mesoderm and endoderm fates, these cells retain their pluripotency (Tsakiridis et al., 2014). In contrast, we find that a significant fraction of the cells labeled by our *Brachyury* reporter has lost pluripotency, as indicated by the inability to establish EpiSC colonies or to contribute to EBs. In support of this, our gene expression data indicate the presence of cells committed to a definitive endoderm fate in EpiSC cultures. The differences in our results may be explained by the *Brachyury* reporters used; the T-GFP reporter is targeted into the endogenous *Brachyury* locus and faithfully replicates its expression (Fehling et al., 2003). In contrast, the Tps/tb-RED reporter used by Tsakiridis et al. (2014) fails to recapitulate *Brachyury* expression in the anterior streak region which, importantly, is the source of definitive endoderm precursors (Clements et al., 1996). Therefore, while the T-GFP-labeled population would include the cells that have lost pluripotency because they committed to a definitive endoderm state, the Tps/tb-RED reporter would not identify this population.

Recently, there has been debate about the nature of the trophoblast-committed cells induced by BMP4 in hESCs, with one study reporting that these cells represent a subpopulation of mesodermal cells that go through a BRACHYURY-positive state (Bernardo et al., 2011). However, the absence of BRACHYURY and other mesendodermal and mesodermal markers in our BMP4+IWP2-differentiated trophoblast cells argues against a mesodermal character.

EXPERIMENTAL PROCEDURES

Statistics

All data are presented as mean ± SEM. Technical replicates are meant unless further specified; p values < 0.05 determined using Student's t test were considered significant.

Cell Culture

EpiSCs were cultured on gelatin and fetal calf serum-coated plates in N2B27 supplemented with 20 ng/ml ACTIVIN A and 12 ng/ml FGF2 (Peprotech). H1 and H9 hESCs were cultured on MEFs in Dulbecco's modified Eagle's medium/F12 supplemented with 20% knockout serum replacement and 10 ng/ml human FGF2 (Millipore). Feeder free culture was done on Matrigel (BD) in mTeSR1 medium (StemCell Technologies). Media, recombinant proteins, and small molecules were changed daily.

Animal Experiments

All animal experiments were conducted after approval by the Erasmus MC animal ethical committee.

Transcriptome Analysis

Total RNA from GFP9 EpiSCs was prepared using TriPure (Roche), converted to biotin-labeled cRNA, hybridized to Affymetrix Mouse Genome 430 2.0 Arrays, and analyzed with the Affymetrix GeneChip Scanner 3000. RNA-Seq was performed at the Erasmus MC Center for Biomics using the Illumina HiSeq platform. We combined Illumina BeadArray gene expression data (Kojima et al., 2014) with our microarray data using a similar approach as described (Heider and Alt, 2013). Microarray (GSE62155) and RNA-Seq (GSE62205) data are available in Gene Expression Omnibus (GEO). Further details are provided in the Supplemental Experimental Procedures.

SUPPLEMENTAL INFORMATION

Supplemental Information includes Supplemental Experimental Procedures, five figures, and five tables and can be found with this article online at http://dx.doi.org/10.1016/j.stemcr.2014.11.007.

ACKNOWLEDGMENTS

129S2C1a EpiSCs were donated by L. Vallier, GOF18 EpiSCs by H.R. Schöler, and T-GFP ESCs by G. Keller. DtB was supported by NWO ECHO.10.B1.064, TI Pharma D5-402, Marie Curie FP7-PEOPLE-2009-RG-256560, ZonMW 911-09-036 and FES NIRM (Dutch Innovation Award), HvdW by NGI Zenith 93511036, and SP by LSBR 1040, ZonMW TOP 40-00812-98-12128, and EU fp7 THALAMOSS 306201.

Received: May 29, 2014
Revised: November 26, 2014
Accepted: November 26, 2014
Published: December 24, 2014

REFERENCES

Bakre, M.M., Hoi, A., Mong, J.C., Koh, Y.Y., Wong, K.Y., and Stanton, L.W. (2007). Generation of multipotential mesendodermal progenitors from mouse embryonic stem cells via sustained Wnt pathway activation. J. Biol. Chem. *282*, 31703–31712.

Ben-Haim, N., Lu, C., Guzman-Ayala, M., Pescatore, L., Mesnard, D., Bischofberger, M., Naef, F., Robertson, E.J., and Constam, D.B. (2006). The nodal precursor acting via activin receptors induces mesoderm by maintaining a source of its convertases and BMP4. Dev. Cell *11*, 313–323.

Bernardo, A.S., Faial, T., Gardner, L., Niakan, K.K., Ortmann, D., Senner, C.E., Callery, E.M., Trotter, M.W., Hemberger, M., Smith, J.C., et al. (2011). BRACHYURY and CDX2 mediate BMP-induced differentiation of human and mouse pluripotent stem cells into embryonic and extraembryonic lineages. Cell Stem Cell *9*, 144–155.

Bernemann, C., Greber, B., Ko, K., Sterneckert, J., Han, D.W., Araúzo-Bravo, M.J., and Schöler, H.R. (2011). Distinct developmental ground states of epiblast stem cell lines determine different pluripotency features. Stem Cells *29*, 1496–1503.

Blauwkamp, T.A., Nigam, S., Ardehali, R., Weissman, I.L., and Nusse, R. (2012). Endogenous Wnt signalling in human embryonic stem cells generates an equilibrium of distinct lineage-specified progenitors. Nat Commun *3*, 1070.

Brons, I.G., Smithers, L.E., Trotter, M.W., Rugg-Gunn, P., Sun, B., Chuva de Sousa Lopes, S.M., Howlett, S.K., Clarkson, A., Ahrlund-Richter, L., Pedersen, R.A., and Vallier, L. (2007). Derivation of pluripotent epiblast stem cells from mammalian embryos. Nature *448*, 191–195.

Chen, B., Dodge, M.E., Tang, W., Lu, J., Ma, Z., Fan, C.W., Wei, S., Hao, W., Kilgore, J., Williams, N.S., et al. (2009). Small molecule-mediated disruption of Wnt-dependent signaling in tissue regeneration and cancer. Nat. Chem. Biol. *5*, 100–107.

Clements, D., Taylor, H.C., Herrmann, B.G., and Stott, D. (1996). Distinct regulatory control of the Brachyury gene in axial and non-axial mesoderm suggests separation of mesoderm lineages early in mouse gastrulation. Mech. Dev. *56*, 139–149.

D'Amour, K.A., Bang, A.G., Eliazer, S., Kelly, O.G., Agulnick, A.D., Smart, N.G., Moorman, M.A., Kroon, E., Carpenter, M.K., and Baetge, E.E. (2006). Production of pancreatic hormone-expressing endocrine cells from human embryonic stem cells. Nat. Biotechnol. *24*, 1392–1401.

Davidson, K.C., Adams, A.M., Goodson, J.M., McDonald, C.E., Potter, J.C., Berndt, J.D., Biechele, T.L., Taylor, R.J., and Moon, R.T. (2012). Wnt/β-catenin signaling promotes differentiation, not self-renewal, of human embryonic stem cells and is repressed by Oct4. Proc. Natl. Acad. Sci. USA *109*, 4485–4490.

Drukker, M., Tang, C., Ardehali, R., Rinkevich, Y., Seita, J., Lee, A.S., Mosley, A.R., Weissman, I.L., and Soen, Y. (2012). Isolation of primitive endoderm, mesoderm, vascular endothelial and trophoblast progenitors from human pluripotent stem cells. Nat. Biotechnol. *30*, 531–542.

Fehling, H.J., Lacaud, G., Kubo, A., Kennedy, M., Robertson, S., Keller, G., and Kouskoff, V. (2003). Tracking mesoderm induction and its specification to the hemangioblast during embryonic stem cell differentiation. Development *130*, 4217–4227.

Frank, S., Zhang, M., Schöler, H.R., and Greber, B. (2012). Small molecule-assisted, line-independent maintenance of human pluripotent stem cells in defined conditions. PLoS ONE *7*, e41958.

Gadue, P., Huber, T.L., Paddison, P.J., and Keller, G.M. (2006). Wnt and TGF-beta signaling are required for the induction of an in vitro model of primitive streak formation using embryonic stem cells. Proc. Natl. Acad. Sci. USA *103*, 16806–16811.

Gardner, R.L., Lyon, M.F., Evans, E.P., and Burtenshaw, M.D. (1985). Clonal analysis of X-chromosome inactivation and the origin of the germ line in the mouse embryo. J. Embryol. Exp. Morphol. *88*, 349–363.

Greber, B., Wu, G., Bernemann, C., Joo, J.Y., Han, D.W., Ko, K., Tapia, N., Sabour, D., Sterneckert, J., Tesar, P., and Schöler, H.R. (2010). Conserved and divergent roles of FGF signaling in mouse epiblast stem cells and human embryonic stem cells. Cell Stem Cell *6*, 215–226.

Gu, G., Wells, J.M., Dombkowski, D., Preffer, F., Aronow, B., and Melton, D.A. (2004). Global expression analysis of gene regulatory pathways during endocrine pancreatic development. Development *131*, 165–179.

Haegel, H., Larue, L., Ohsugi, M., Fedorov, L., Herrenknecht, K., and Kemler, R. (1995). Lack of beta-catenin affects mouse development at gastrulation. Development *121*, 3529–3537.

Han, D.W., Tapia, N., Joo, J.Y., Greber, B., Araúzo-Bravo, M.J., Bernemann, C., Ko, K., Wu, G., Stehling, M., Do, J.T., and Schöler, H.R. (2010). Epiblast stem cell subpopulations represent mouse embryos of distinct pregastrulation stages. Cell *143*, 617–627.

Hao, J., Li, T.G., Qi, X., Zhao, D.F., and Zhao, G.Q. (2006). WNT/beta-catenin pathway up-regulates Stat3 and converges on LIF to prevent differentiation of mouse embryonic stem cells. Dev. Biol. *290*, 81–91.

Heider, A., and Alt, R. (2013). virtualArray: a R/bioconductor package to merge raw data from different microarray platforms. BMC Bioinformatics *14*, 75.

Hou, J., Charters, A.M., Lee, S.C., Zhao, Y., Wu, M.K., Jones, S.J., Marra, M.A., and Hoodless, P.A. (2007). A systematic screen for genes expressed in definitive endoderm by Serial Analysis of Gene Expression (SAGE). BMC Dev. Biol. *7*, 92.

Huang, Y., Osorno, R., Tsakiridis, A., and Wilson, V. (2012). In Vivo differentiation potential of epiblast stem cells revealed by chimeric embryo formation. Cell Rep *2*, 1571–1578.

Huelsken, J., Vogel, R., Brinkmann, V., Erdmann, B., Birchmeier, C., and Birchmeier, W. (2000). Requirement for beta-catenin in anterior-posterior axis formation in mice. J. Cell Biol. *148*, 567–578.

Kojima, Y., Kaufman-Francis, K., Studdert, J.B., Steiner, K.A., Power, M.D., Loebel, D.A., Jones, V., Hor, A., de Alencastro, G., Logan, G.J., et al. (2014). The transcriptional and functional properties of mouse epiblast stem cells resemble the anterior primitive streak. Cell Stem Cell *14*, 107–120.

Lako, M., Lindsay, S., Lincoln, J., Cairns, P.M., Armstrong, L., and Hole, N. (2001). Characterisation of Wnt gene expression during the differentiation of murine embryonic stem cells in vitro: role of Wnt3 in enhancing haematopoietic differentiation. Mech. Dev. *103*, 49–59.

Lindsley, R.C., Gill, J.G., Kyba, M., Murphy, T.L., and Murphy, K.M. (2006). Canonical Wnt signaling is required for development of embryonic stem cell-derived mesoderm. Development *133*, 3787–3796.

Liu, P., Wakamiya, M., Shea, M.J., Albrecht, U., Behringer, R.R., and Bradley, A. (1999). Requirement for Wnt3 in vertebrate axis formation. Nat. Genet. *22*, 361–365.

Loh, K.M., Ang, L.T., Zhang, J., Kumar, V., Ang, J., Auyeong, J.Q., Lee, K.L., Choo, S.H., Lim, C.Y., Nichane, M., et al. (2014). Efficient endoderm induction from human pluripotent stem cells by logically directing signals controlling lineage bifurcations. Cell Stem Cell *14*, 237–252.

McLean, A.B., D'Amour, K.A., Jones, K.L., Krishnamoorthy, M., Kulik, M.J., Reynolds, D.M., Sheppard, A.M., Liu, H., Xu, Y., Baetge, E.E., and Dalton, S. (2007). Activin a efficiently specifies definitive endoderm from human embryonic stem cells only when phosphatidylinositol 3-kinase signaling is suppressed. Stem Cells *25*, 29–38.

Mohamed, O.A., Clarke, H.J., and Dufort, D. (2004). Beta-catenin signaling marks the prospective site of primitive streak formation in the mouse embryo. Dev. Dyn. *231*, 416–424.

Nichols, J., and Smith, A. (2009). Naive and primed pluripotent states. Cell Stem Cell *4*, 487–492.

Nostro, M.C., Cheng, X., Keller, G.M., and Gadue, P. (2008). Wnt, activin, and BMP signaling regulate distinct stages in the developmental pathway from embryonic stem cells to blood. Cell Stem Cell *2*, 60–71.

Ogaki, S., Harada, S., Shiraki, N., Kume, K., and Kume, S. (2011). An expression profile analysis of ES cell-derived definitive endodermal cells and Pdx1-expressing cells. BMC Dev. Biol. *11*, 13.

Ogawa, K., Nishinakamura, R., Iwamatsu, Y., Shimosato, D., and Niwa, H. (2006). Synergistic action of Wnt and LIF in maintaining pluripotency of mouse ES cells. Biochem. Biophys. Res. Commun. *343*, 159–166.

Ohtsuka, S., Nishikawa-Torikai, S., and Niwa, H. (2012). E-cadherin promotes incorporation of mouse epiblast stem cells into normal development. PLoS ONE *7*, e45220.

Pera, M.F., Andrade, J., Houssami, S., Reubinoff, B., Trounson, A., Stanley, E.G., Ward-van Oostwaard, D., and Mummery, C. (2004). Regulation of human embryonic stem cell differentiation by BMP-2 and its antagonist noggin. J. Cell Sci. *117*, 1269–1280.

Pfister, S., Steiner, K.A., and Tam, P.P. (2007). Gene expression pattern and progression of embryogenesis in the immediate post-implantation period of mouse development. Gene Expr. Patterns *7*, 558–573.

Rivera-Pérez, J.A., and Magnuson, T. (2005). Primitive streak formation in mice is preceded by localized activation of Brachyury and Wnt3. Dev. Biol. *288*, 363–371.

Singla, D.K., Schneider, D.J., LeWinter, M.M., and Sobel, B.E. (2006). wnt3a but not wnt11 supports self-renewal of embryonic stem cells. Biochem. Biophys. Res. Commun. *345*, 789–795.

Stewart, M.H., Bossé, M., Chadwick, K., Menendez, P., Bendall, S.C., and Bhatia, M. (2006). Clonal isolation of hESCs reveals heterogeneity within the pluripotent stem cell compartment. Nat. Methods *3*, 807–815.

Subramanian, A., Tamayo, P., Mootha, V.K., Mukherjee, S., Ebert, B.L., Gillette, M.A., Paulovich, A., Pomeroy, S.L., Golub, T.R., Lander, E.S., and Mesirov, J.P. (2005). Gene set enrichment analysis: a knowledge-based approach for interpreting genome-wide expression profiles. Proc. Natl. Acad. Sci. USA *102*, 15545–15550.

Sumi, T., Tsuneyoshi, N., Nakatsuji, N., and Suemori, H. (2008). Defining early lineage specification of human embryonic stem cells by the orchestrated balance of canonical Wnt/beta-catenin, Activin/Nodal and BMP signaling. Development *135*, 2969–2979.

Sumi, T., Oki, S., Kitajima, K., and Meno, C. (2013). Epiblast ground state is controlled by canonical Wnt/β-catenin signaling in the postimplantation mouse embryo and epiblast stem cells. PLoS ONE *8*, e63378.

Tada, S., Era, T., Furusawa, C., Sakurai, H., Nishikawa, S., Kinoshita, M., Nakao, K., Chiba, T., and Nishikawa, S. (2005). Characterization of mesendoderm: a diverging point of the definitive endoderm and mesoderm in embryonic stem cell differentiation culture. Development *132*, 4363–4374.

ten Berge, D., Koole, W., Fuerer, C., Fish, M., Eroglu, E., and Nusse, R. (2008). Wnt signaling mediates self-organization and axis formation in embryoid bodies. Cell Stem Cell *3*, 508–518.

ten Berge, D., Kurek, D., Blauwkamp, T., Koole, W., Maas, A., Eroglu, E., Siu, R.K., and Nusse, R. (2011). Embryonic stem cells require Wnt proteins to prevent differentiation to epiblast stem cells. Nat. Cell Biol. *13*, 1070–1075.

Tesar, P.J., Chenoweth, J.G., Brook, F.A., Davies, T.J., Evans, E.P., Mack, D.L., Gardner, R.L., and McKay, R.D. (2007). New cell lines from mouse epiblast share defining features with human embryonic stem cells. Nature *448*, 196–199.

Tortelote, G.G., Hernández-Hernández, J.M., Quaresma, A.J., Nickerson, J.A., Imbalzano, A.N., and Rivera-Pérez, J.A. (2013). Wnt3 function in the epiblast is required for the maintenance but not the initiation of gastrulation in mice. Dev. Biol. *374*, 164–173.

Tsakiridis, A., Huang, Y., Blin, G., Skylaki, S., Wymeersch, F., Osorno, R., Economou, C., Karagianni, E., Zhao, S., Lowell, S., and Wilson, V. (2014). Distinct Wnt-driven primitive streak-like populations reflect in vivo lineage precursors. Development *141*, 1209–1221.

Waldrip, W.R., Bikoff, E.K., Hoodless, P.A., Wrana, J.L., and Robertson, E.J. (1998). Smad2 signaling in extraembryonic tissues determines anterior-posterior polarity of the early mouse embryo. Cell *92*, 797–808.

Winnier, G., Blessing, M., Labosky, P.A., and Hogan, B.L. (1995). Bone morphogenetic protein-4 is required for mesoderm formation and patterning in the mouse. Genes Dev. *9*, 2105–2116.

Xu, R.H., Chen, X., Li, D.S., Li, R., Addicks, G.C., Glennon, C., Zwaka, T.P., and Thomson, J.A. (2002). BMP4 initiates human embryonic stem cell differentiation to trophoblast. Nat. Biotechnol. *20*, 1261–1264.

Ying, Q.L., Nichols, J., Chambers, I., and Smith, A. (2003). BMP induction of Id proteins suppresses differentiation and sustains embryonic stem cell self-renewal in collaboration with STAT3. Cell *115*, 281–292.

Zhang, K., Li, L., Huang, C., Shen, C., Tan, F., Xia, C., Liu, P., Rossant, J., and Jing, N. (2010). Distinct functions of BMP4 during different stages of mouse ES cell neural commitment. Development *137*, 2095–2105.

Stem Cell Reports, Volume *4*

Supplemental Information

Endogenous WNT Signals Mediate BMP-Induced and Spontaneous Differentiation of Epiblast Stem Cells and Human Embryonic Stem Cells

Dorota Kurek, Alex Neagu, Melodi Tastemel, Nesrin Tüysüz, Johannes Lehmann, Harmen J.G. van de Werken, Sjaak Philipsen, Reinier van der Linden, Alex Maas, Wilfred F.J. van IJcken, Micha Drukker, and Derk ten Berge

Supplemental Figure Legends

Figure S1, related to Figure 1. (A-D) T-GFP ESCs were differentiated into EpiSCs by culture in FGF2 and ACTIVIN for 4 passages. The cells acquired the characteristic flattened EpiSC morphology (A), lost expression of the ESC markers *Stella* and *Rex1*, and gained expression of the EpiSC markers *Fgf5* and *Dnmt3b* (B). To verify that the cells had truly differentiated, we transferred them back into ESC conditions as a single cell suspension. On average 8 per 100,000 cells regenerated an ESC colony (n=3) (C), in line with the reversal efficiency of epiblast-derived EpiSCs (Bernemann et al., 2011; Greber et al., 2010), indicating complete differentiation. Teratoma assays demonstrated that the cells retained their pluripotency as they produced teratomas containing derivatives of all 3 germ layers (D). E) Immunofluorescence images of 129S2C1a EpiSCs cultured for 3 days with the indicated factors and immunostained as indicated (blue: DAPI). F) Flow cytometry plots of T-GFP EpiSCs treated with WNT3A and IWP2 and analyzed for T-GFP and SSEA1. G) Plot showing the expansion of SSEA1-positive 129S2C1a EpiSCs in the indicated conditions (mean +/- s.e.m.; n=3 independent experiments). Scale bar: 200 μm (A), 100 μm (D,E).

Figure S1

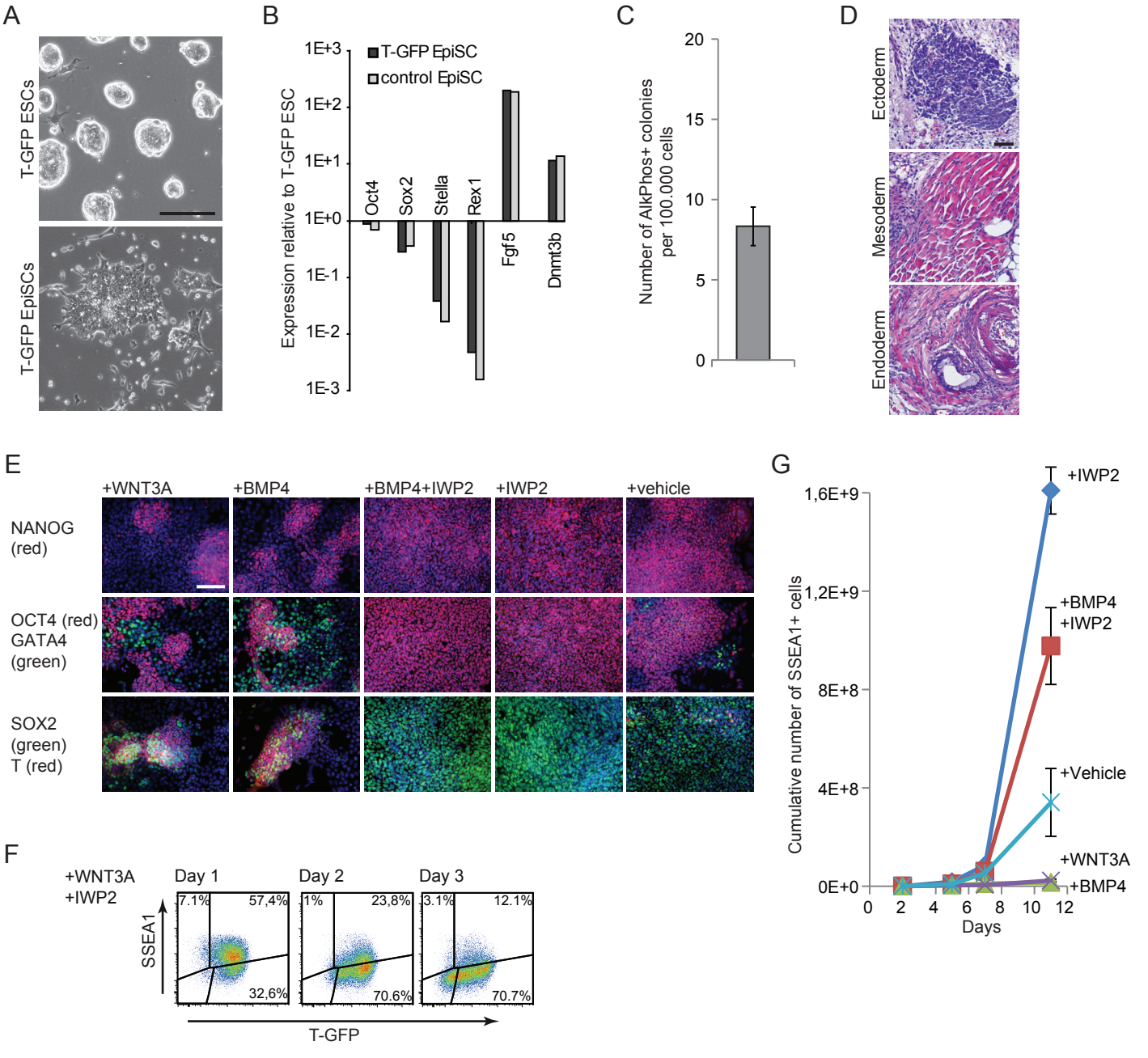
A
T-GFP ESCs
T-GFP EpiSCs
B
T-GFP EpiSC
control EpiSC
Expression relative to T-GFP ESC
1E+3
1E+2
1E+1
1E+0
1E-1
1E-2
1E-3
Oct4
Sox2
Stella
Rex1
Fgf5
Dnmt3b
C
Number of AlkPhos+ colonies per 100.000 cells
20
15
10
5
0
D
Ectoderm
Mesoderm
Endoderm
E
+WNT3A
+BMP4
+BMP4+IWP2
+IWP2
+vehicle
NANOG (red)
OCT4 (red) GATA4 (green)
SOX2 (green) T (red)
F
+WNT3A +IWP2
Day 1
Day 2
Day 3
SSEA1
T-GFP
7.1%
57,4%
32,6%
1%
23,8%
70.6%
3.1%
12.1%
70.7%
G
Cumulative number of SSEA1+ cells
1,6E+9
1,2E+9
8E+8
4E+8
0E+0
0
2
4
6
8
10
12
Days
+IWP2
+BMP4 +IWP2
+Vehicle
+WNT3A
+BMP4

Figure S2, related to Figure 2. A) Expression level of *Wnt* genes in 129S2C1a EpiSCs relative to *Gapdh* (mean +/- s.e.m., n=3; ND, not detected). B) Representative examples of EpiSC colonies obtained from sorted T-GFP EpiSCs, stained for NANOG (red), and quantified in Figure 2A. All colonies stained positive for NANOG, while NANOG-negative cells only formed dispersed clusters. C) Gating strategy relating to Figure 2A.D) Gating strategy relating to Figure 2B. E) Flow cytometry histograms showing several EpiSC lines treated for 3 days with the indicated factors and analyzed for SSEA1. F) Heat map of selected gene expression levels of GFP9 EpiSCs cultured in the presence or absence of IWP2 and analyzed by microarray. Scale bar: 100 μm.

Figure S2

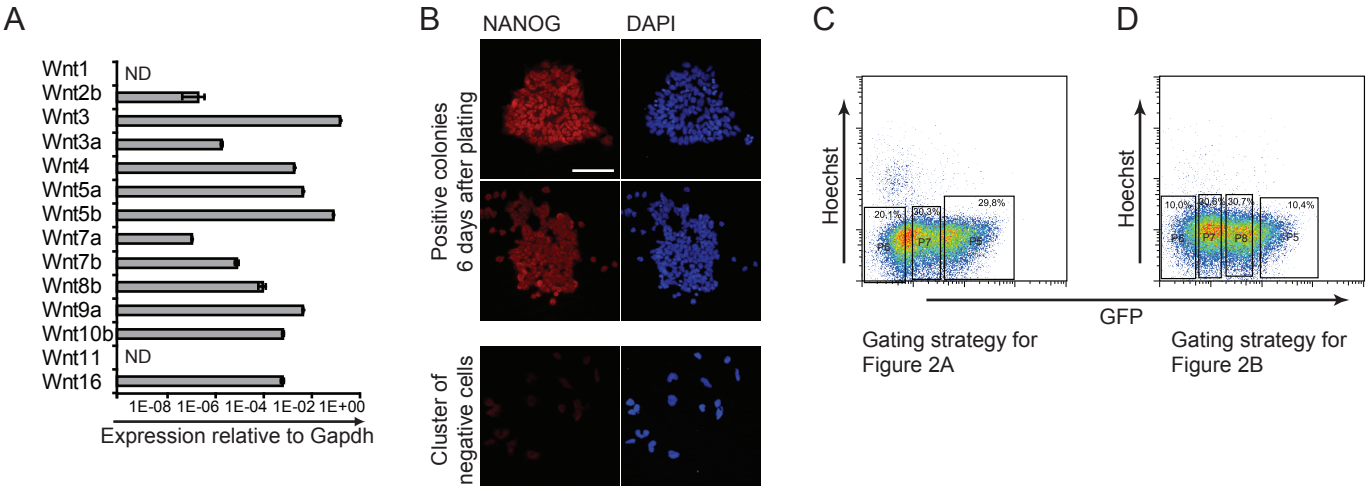
A
Wnt1
Wnt2b
Wnt3
Wnt3a
Wnt4
Wnt5a
Wnt5b
Wnt7a
Wnt7b
Wnt8b
Wnt9a
Wnt10b
Wnt11
Wnt16
ND
ND
1E-08 1E-06 1E-04 1E-02 1E+00
Expression relative to Gapdh
B
NANOG
DAPI
Positive colonies 6 days after plating
Cluster of negative cells
C
Hoechst
GFP
Gating strategy for Figure 2A
D
Hoechst
Gating strategy for Figure 2B

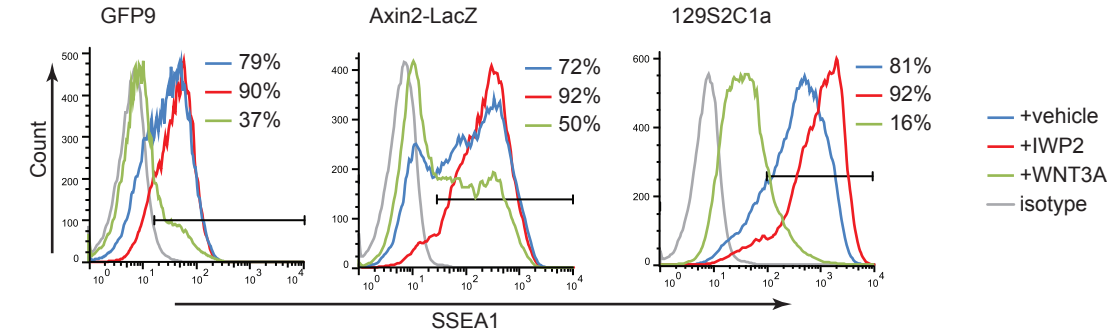
E
GFP9
Axin2-LacZ
129S2C1a
Count
79%
90%
37%
72%
92%
50%
81%
92%
16%
+vehicle
+IWP2
+WNT3A
isotype
SSEA1

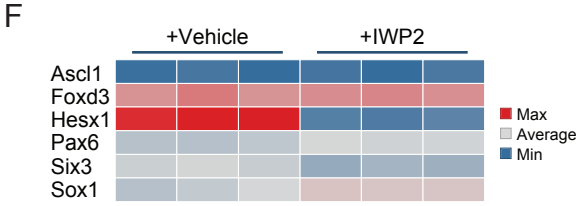
F
+Vehicle
+IWP2
Ascl1
Foxd3
Hesx1
Pax6
Six3
Sox1
Max
Average
Min

Figure S3, related to Figure 3. A) Immunofluorescence images of sections of X-gal stained chimeras immunostained as indicated. B) Flow cytometry plots of GOF18 EpiSCs cultured at indicated conditions for 4 passages and analyzed for SSEA1 and GFP (mean +/- s.e.m.; n=3 independent experiments). C) Flow cytometry histograms showing percentage of GFP positive cells from GFP-positive and GFP-negative GOF18 EpiSCs analyzed 4 and 18 days after sorting. Scale bar: 50 μm.

Figure S3

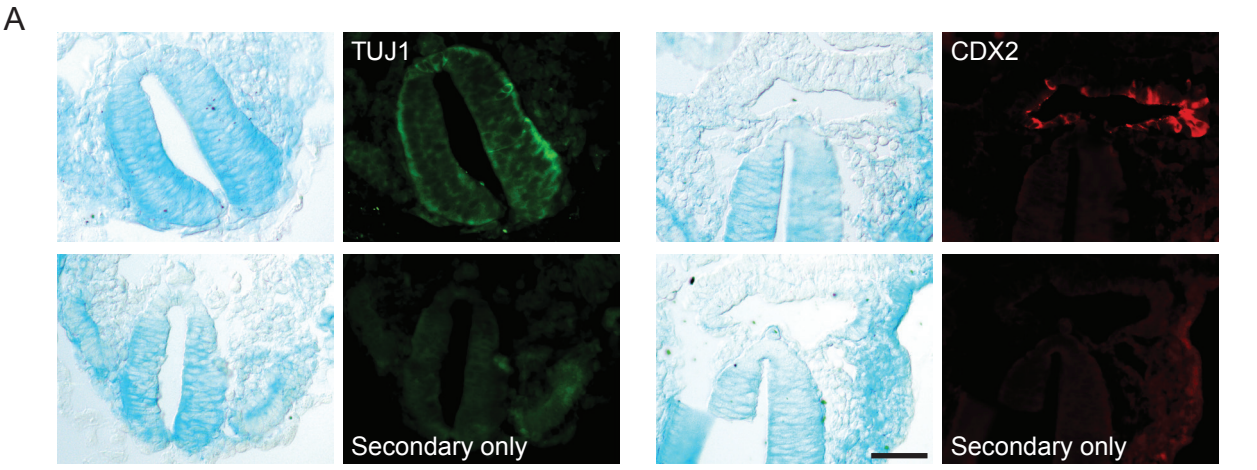
A
TUJ1
CDX2
Secondary only
Secondary only

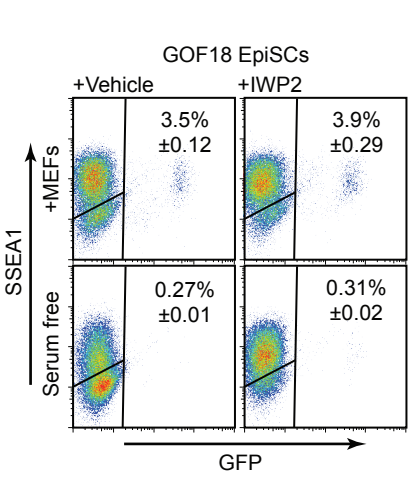
B
GOF18 EpiSCs
+Vehicle
+IWP2
3.5%
±0.12
3.9%
±0.29
0.27%
±0.01
0.31%
±0.02
SSEA1
+MEFs
Serum free
GFP

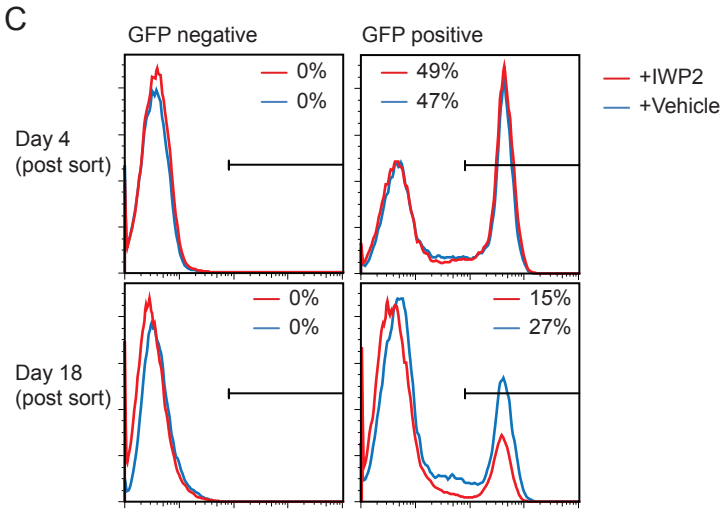
C
GFP negative
GFP positive
Day 4
(post sort)
Day 18
(post sort)
0%
0%
49%
47%
0%
0%
15%
27%
+IWP2
+Vehicle

Figure S4, related to Figure 4. A) Representative phase contrast images of H9 (on MEFs) or H1 (mTESR1) hESCs cultured for 6 days at the indicated conditions. Arrows indicate differentiating areas of the colonies. B,C) Immunofluorescence images of H1 (B) or H9 (C) hESCs cultured for 6 days with the indicated factors and immunostained as indicated (blue: DAPI). D) Flow cytometry histograms showing H9 hESCs cultured in the indicated conditions for 7 days and analyzed for NANOG, OCT4 and SOX2. E) Real-time RT-PCR gene expression profile of H9 hESCs cultured for 6 days in the presence of IWP2, plotted relative to cells maintained in the absence of IWP2 (+/- s.e.m.; n=3). F) Percentage of H9 hESCs triple positive for NANOG, OCT4 and SOX2, cultured using the indicated conditions and procedures (mean +/- s.e.m.; n=3 independent experiments). G) Percentage of H9 hESCs expressing SSEA1 cultured using the indicated conditions and procedures (mean +/- s.e.m.; n=3 independent experiments). H) Flow cytometry histograms for SSEA1 and pluripotency transcription factors in H9 and H1 hESCs cultured using the indicated conditions and procedures. Pluripotency factor expression was determined either at day 19 (H9) or day 21 (H1). I) H9 or H1 hESCs were cultured in the presence of IWP2 for 10 passages and then used to establish teratomas. Hematoxylin and eosin staining shows the presence of all 3 germ layers in the teratomas. Scale bar: 200 μm (A,C and I), 100 μm (B).

Figure S4

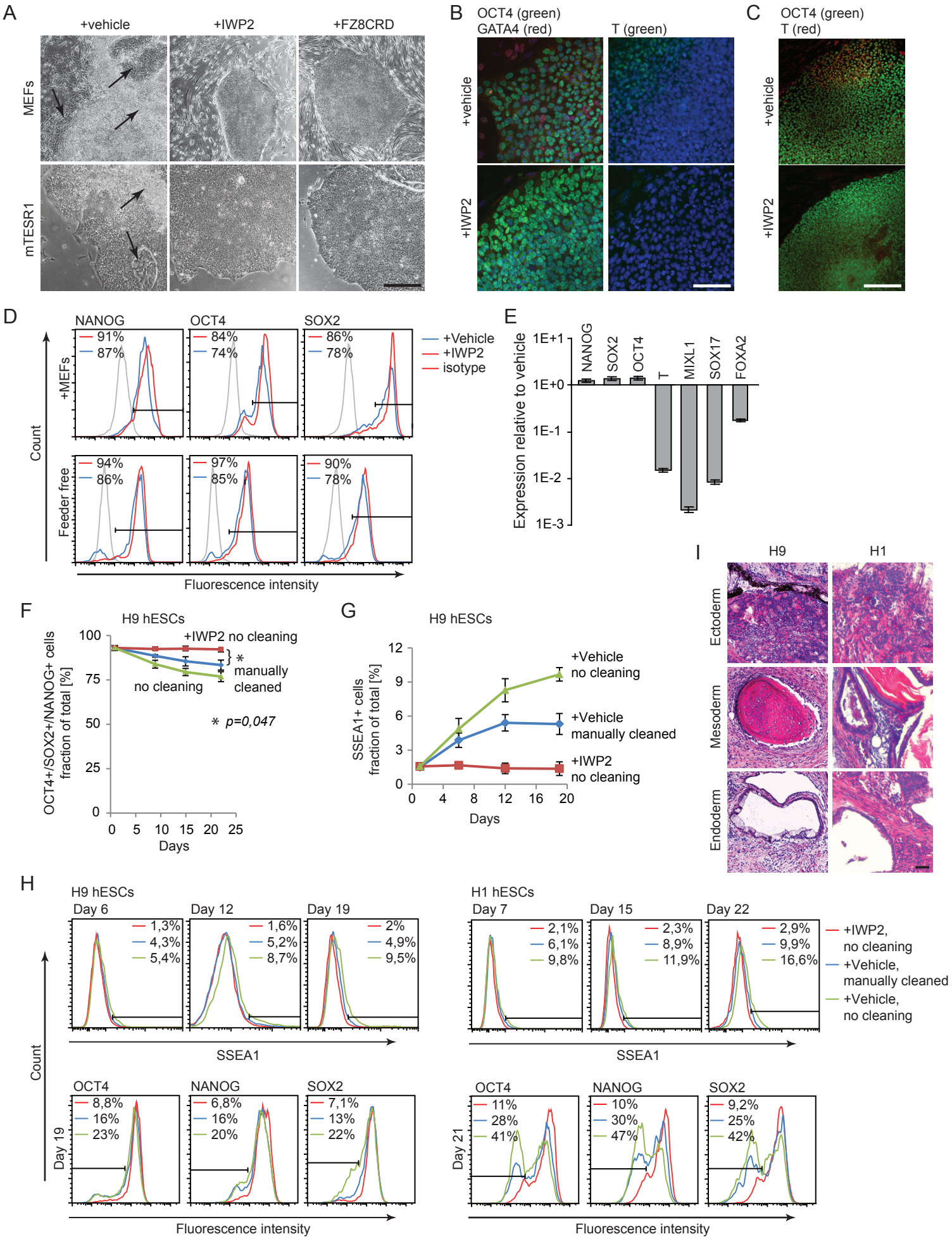
A
+vehicle
+IWP2
+FZ8CRD
MEFs
mTESR1
B
OCT4 (green)
GATA4 (red)
T (green)
+vehicle
+IWP2
C
OCT4 (green)
T (red)
+vehicle
+IWP2
D
NANOG
OCT4
SOX2
91%
87%
84%
74%
86%
78%
94%
86%
97%
85%
90%
78%
+MEFs
Feeder free
Count
+Vehicle
+IWP2
isotype
Fluorescence intensity
E
Expression relative to vehicle
1E+1
1E+0
1E-1
1E-2
1E-3
NANOG
SOX2
OCT4
T
MIXL1
SOX17
FOXA2
F
H9 hESCs
OCT4+/SOX2+/NANOG+ cells
fraction of total [%]
100
75
50
25
0
+IWP2 no cleaning
manually
cleaned
no cleaning
* p=0,047
0 5 10 15 20 25
Days
G
H9 hESCs
SSEA1+ cells
fraction of total [%]
12
9
6
3
0
+Vehicle
no cleaning
+Vehicle
manually cleaned
+IWP2
no cleaning
0 4 8 12 16 20
Days
I
H9
H1
Ectoderm
Mesoderm
Endoderm
H
H9 hESCs
Day 6
Day 12
Day 19
1,3%
4,3%
5,4%
1,6%
5,2%
8,7%
2%
4,9%
9,5%
SSEA1
Count
OCT4
NANOG
SOX2
8,8%
16%
23%
6,8%
16%
20%
7,1%
13%
22%
Day 19
Fluorescence intensity
H1 hESCs
Day 7
Day 15
Day 22
2,1%
6,1%
9,8%
2,3%
8,9%
11,9%
2,9%
9,9%
16,6%
SSEA1
+IWP2,
no cleaning
+Vehicle,
manually cleaned
+Vehicle,
no cleaning
OCT4
NANOG
SOX2
11%
28%
41%
10%
30%
47%
9,2%
25%
42%
Day 21
Fluorescence intensity

Figure S5, related to Figure 5. A) Immunofluorescence images of H1 hESCs cultured with the indicated factors for 7 days and immunostained as indicated (blue: DAPI). B) Flow cytometry plots from the experiment shown in Figure 5A, showing H1 hESCs cultured with the indicated factors for 3 or 6 days and analyzed for ROR2. C) Flow cytometry histograms showing H1 hESCs cultured with the indicated factors for 4 and 12 days and analyzed for NANOG, OCT4 and SOX2. D) Flow cytometry plots from the experiment shown in Figure 5E, showing H1 hESCs cultured with the indicated factors for 3 or 6 days and analyzed for APA. E) Flow cytometry histograms showing H1 hESCs differentiated with BMP4 in the presence of IWP2 for 5 and 7 days and analyzed for APA (mean +/- s.e.m.; n=3 independent experiments). Scale bar: 100 μm.

Figure S5

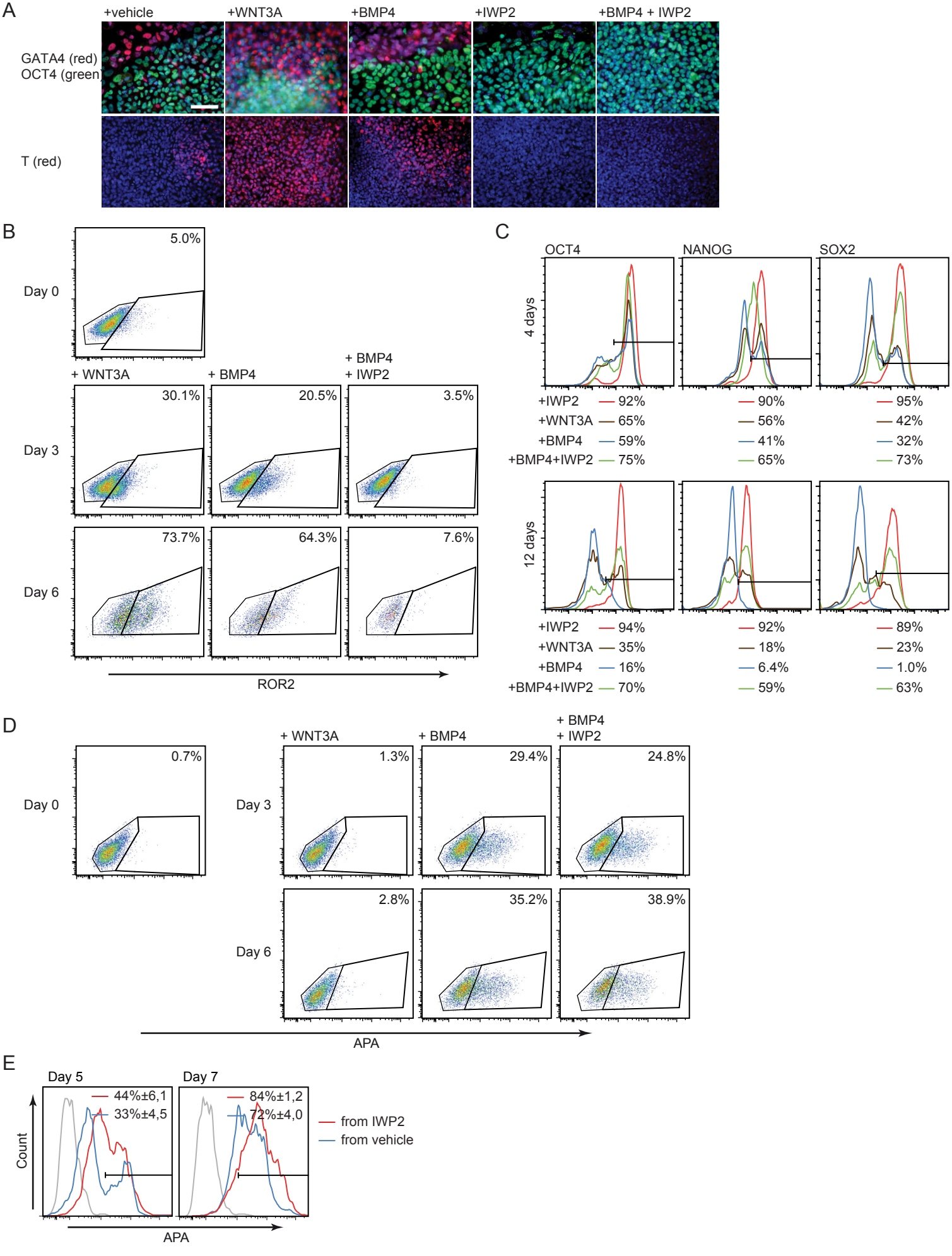
A
+vehicle
+WNT3A
+BMP4
+IWP2
+BMP4 + IWP2
GATA4 (red)
OCT4 (green)
T (red)
B
Day 0
5.0%
+ WNT3A
+ BMP4
+ BMP4
+ IWP2
Day 3
30.1%
20.5%
3.5%
Day 6
73.7%
64.3%
7.6%
ROR2
C
OCT4
NANOG
SOX2
4 days
+IWP2 92% 90% 95%
+WNT3A 65% 56% 42%
+BMP4 59% 41% 32%
+BMP4+IWP2 75% 65% 73%
12 days
+IWP2 94% 92% 89%
+WNT3A 35% 18% 23%
+BMP4 16% 6.4% 1.0%
+BMP4+IWP2 70% 59% 63%
D
Day 0
0.7%
+ WNT3A
+ BMP4
+ BMP4
+ IWP2
Day 3
1.3%
29.4%
24.8%
Day 6
2.8%
35.2%
38.9%
APA
E
Day 5
Day 7
44%±6,1
33%±4,5
84%±1,2
72%±4,0
from IWP2
from vehicle
Count
APA

Supplemental Table Legends

Table S1. Genes Differentially Expressed between EpiSCs Maintained in the Presence or Absence of IWP2, Related to Figure 2.
This table uses a threshold value of 0.05 for false discovery rate-adjusted p value and minimum fold change of 2. The list contains 515 probe sets representing 408 unique gene symbols.

Table S2. Gene Set Enrichment Analysis for Gastrulation Markers in EpiSCs Maintained in the Absence versus the Presence of IWP2, Related to Figure 2.

Table S3. Gene Set Enrichment Analysis for Definitive Endoderm Markers in EpiSCs Maintained in the Absence versus the Presence of IWP2, Related to Figure 2.

Table S4. Gene Set Enrichment Analysis for Markers Expressed in Endoderm and Absent from Mesoderm and Ectoderm in EpiSCs Maintained in the Absence versus the Presence of IWP2, Related to Figure 2.

Table S5. Gene Set Enrichment Analysis for Markers Expressed in Mesoderm and Ectoderm and Absent from Endoderm in EpiSCs Maintained in the Absence versus the Presence of IWP2, Related to Figure 2.

Supplemental Experimental Procedures

Cell culture. Epiblast stem cells (EpiSCs) were cultured on gelatin and fetal calf serum coated plates in EpiSC medium: N2B27 medium supplemented with 20 ng/ml ActivinA and 12 ng/ml bFGF (both Peprotech). N2B27 medium consisted of one volume DMEM/F12 combined with one volume Neurobasal medium, supplemented with 0.5% N2 Supplement, 1% B27 Supplement, 0.033% BSA 7.5% solution, 50 μM β-mercaptoethanol, 2 mM Glutamax, 100 U/ml penicillin and 100 μg/ml streptomycin (all from Invitrogen). EpiSCs were passaged 1:4–1:10 every 3 days by triturating the colonies into small clumps using 0.5 mg/ml collagenase IV (Sigma).

To differentiate EpiSCs from ES cells, trypsinized ES cells were seeded at a density of 10,000 cells/cm^2 on gelatin and FCS coated plates in EpiSC medium supplemented with 1,000 U/ml LIF for the first passage. The cells were then passaged 1:4–1:10 every 3 days as small clumps using 0.5 mg/ml collagenase IV.

To revert EpiSCs to ESCs, EpiSCs were triturated to a single cell suspension in 0.5 mg/ml collagenase IV (Sigma) and seeded at a density of 2,000 cells/cm^2 in EpiSC medium on MEFs supplemented with 10μM the ROCK inhibitor Y-27632 (Stemgent). The next day, the medium was changed to N2B27 medium supplemented with LIF (1,000 U/ml), PD0325901 and CHIR99021. After 4 days the cells were stained for alkaline phosphatase activity using the SCR004 kit (Millipore) and the number of alkaline phosphatase-positive colonies counted.

Mouse ESCs were cultured in N2B27 medium supplemented with 1,000 U/ml LIF (Chemicon) and 250 ng/ml Wnt3a protein on gelatin coated plates.

WA01 (H1) and WA09 (H9) hESCs were cultured on irradiated mouse embryonic fibroblast feeder layers in medium consisting of DMEM/F12 supplemented with 20% Knockout Serum Replacement, 2 mM Glutamax, 1x MEM non-essential amino acids, 50 μM β-mercaptoethanol, 100 U/ml penicillin, 100 μg/ml streptomycin (all from Invitrogen) and supplemented with 10 ng/ml human bFGF (Millipore). For differentiation experiments cells were cultured on a layer of Matrigel (BD Biosciences) in medium consisting of DMEM/F12 supplemented with 20% Serum (HyClone), 2 mM Glutamax, 1x MEM non-essential amino acids, 50 μM β-mercaptoethanol, 100 U/ml penicillin, 100 μg/ml streptomycin (all from Invitrogen) and supplemented with 250 ng/ml Wnt3a, 50 ng/ml BMP4, or 2 μm IWP2, as indicated.

For feeder free culture, hESCs were cultured on a layer of Matrigel (BD Biosciences) in mTeSR1 medium (Stemcells Technologies) or TeSR-E8 medium (Stemcells Technologies).

Media, recombinant proteins and small molecules were changed daily in all experiments except when indicated otherwise. IWP2 (Merck or Stemgent), CHIR99021 (Axon Medchem or Stemgent), PD0325901 (Merck), LDN-193189 (Stemgent) and ROCK inhibitor Y-27632 (Stemgent) were diluted from 2 mM (IWP2), 0.2 mM (LDN-193189) or 10 mM (others) stocks in water (Y-27632) or dimethylsulphoxide (all others), and used at 2, 3, 0.9, 0.2 and 10 μM, respectively. Bmp4 (Invitrogen) was used at 15 ng/ml for EpiSCs, and 50 ng/ml for hESCs. Wnt3a and Fz8CRD proteins were used at 250 and 1,000 ng/ml, respectively. Recombinant mouse Wnt3a protein was produced in Drosophila S2 cells grown in suspension culture, and purified by Blue Sepharose affinity and gel filtration chromatography as described (Willert et al., 2003). Fz8CRD was produced as an Fc fusion protein as described (Hsieh et al., 1999).

Epiblast Stem Cell derivation. Epiblasts were dissected from E6.5 Rosa26-LacZ (Soriano, 1999) or Actin-GFP (Okabe et al., 1997) embryos and collected in DMEM with 10% FCS and 20 mM HEPES. After dissociation into small clumps using a brief trypsin-EDTA treatment, the clumps were plated on a MEF feeder layer in DMEM supplemented with 18% Knockout Serum

Replacement, 2% fetal bovine serum (Hyclone), 1 mM sodium pyruvate, 1x MEM non-essential amino acids, 50 μM β-mercaptoethanol, 100 U ml/1 penicillin, 100 μg ml/1 streptomycin (all from Invitrogen), 12 ng/ml bFGF (Peprotech) and 2 μM IWP2 (Stemgent). Four to seven days after initial plating, the epiblast outgrowths were passaged using 0.5 mg/ml collagenase IV and expand in MEF-containing culture. The MEFs were plated in the presence of 2 μM IWP2 prior to start of derivation or passaging to prevent the accumulation of endogenous Wnt proteins. Usually EpiSCs were transferred to feeder-free N2B27 media after passage 2.

EpiSCs and hESCs self-renewal assays. To quantify self-renewal over multiple passages, EpiSCs or hESCs were initially plated in 12-well plates at 1:10 ratio and the total number of cells was estimated. Every 2-3 days for EpiSCs and 5-7 days for hESCs cells were passaged at ratio that would result to a similar density (between 1:4 to 1:10 ratio) and at the same time cells were stained with SSEA1 or nuclear pluripotency markers for FACS analysis (see FACS marker staining). The cumulative number of positive cells was calculated by multiplying the cell counts by the dilution factor used for passaging.

Teratoma formation. EpiSCs and hESCs were harvested using 0.5 mg/ml collagenase IV (Sigma) and resuspended in PBS or 30% BD Matrigel in PBS (BD Biosciences), respectively. Between $2x10^6$ and $6x10^6$ cells were subcutaneously injected into the flank of NOD/SCID mice. After 5-8 weeks teratomas were removed, fixed in 4% PFA, embedded in paraffin, sectioned and stained with hematoxylin and eosin. All animal procedures were performed in accordance with institutional and national guidelines and regulations, and approved by the Erasmus MC Animal Experiment Committee (DEC).

Blastocyst injection. EpiSCs were recovered by treatment with Enzyme-Free Cell Dissociation Buffer (Gibco), and 10-15 cells were injected into blastocysts collected from C57Bl/6 mice. Blastocysts (10-15 per mouse) were transferred into the uterus of a pseudopregnant mouse and embryos recovered 7 days later.

Embryoid body formation. T-GFP and 7xtcf-GFP ESCs were triturated to a single cell suspension using trypsin-EDTA and resuspended in differentiation medium composed of DMEM plus 15% fetal bovine serum (Hyclone), 1x MEM non-essential amino acids, 50 μM β-mercaptoethanol, 100 U/ml penicillin, 100 μg/ml streptomycin (all from Invitrogen). Hanging drops were prepared from 2000 ESCs per 20 μl drop in differentiation medium. After 3 days embryoid bodies were transferred to low attachment plates for further culture in a shaking incubator. The embryoid bodies were collected at indicated time points and dissociated into single cells using collagenase IV in 5% FCS/PBS (5 minutes in 37°C) and collected for flow cytometry. Following markers were used for staining: SSEA1-PE (eBioscience, 1:50) and CD31-PE-Cy7 (eBioscience, 1:2000) in 5% FCS/PBS for 40 minutes at 4°C. 1μg/ml Hoechst 33258 (Molecular Probes) was used for live/dead cells assessment. Cells were analyzed using a FACSAria III flow cytometer and results analyzed by FlowJo.

Correlation between level of Brachyury reporter and ability to form EpiSC colonies or embryoid bodies. T-GFP EpiSCs were plated in N2B27 medium supplemented ActivinA and bFGF for 3 days, dissociated with 0.5 mg/ml collagenase IV (Sigma) for EpiSC colony formation assay or by 0.25% Trypsin-EDTA for embryoid body formation assay, resuspended in PBS with 10% serum and 1 μg/ml Hoechst 33258, and live cells sorted into 3 or 4 categories based on GFP intensity using a FACSAria III cell sorter (BD Biosciences). The gating strategies are shown in Figures S2D and S2E. Sorted cells were seeded at a density of 3000 or 6000 cells/cm^2 in N2B27 medium supplemented with bFGF, Activin A, IWP2 and ROCK inhibitor. After 6 days the cells were immunostained for Nanog and the number of positive colonies was counted by eye. For

embryoid body formation, 6000 sorted cells per 25 µl droplet were aggregated in hanging drops for 3 days, and the embryoid bodies collected and photographed.

Flow cytometry. For live flow cytometry experiments of EpiSCs, single cell suspensions were made using trypsin-EDTA (5 minutes in 37°C), washed with 5% FCS/PBS, and stained with SSEA1-PE (eBioscience, 1:50) for 40 minutes at 4°C. 1µg/ml Hoechst 33258 or 7AAD was used for live/dead cells assessment. Prior to the time course experiment of T-GFP EpiSCs treated with gastrulation-inducing factors, cells were cultured in the presence of IWP2 for one passage.
For live flow cytometry experiments of hESCs, single cell suspensions were made using Enzyme-Free Cell Dissociation Buffer (Gibco) for 30 min at 37ºC, washed with 5% FCS/PBS and stained with anti-APA or anti-ROR2 as described previously (Drukker et al., 2012). For the nuclear pluripotency markers, EpiSCs and hESCs were stained using Mouse or Human Pluripotent Stem Cell Transcription Factor Analysis Kits (BD Biosciences) according to the manufacturer's protocol. Cells were analyzed using FACSAria III, FACS Fortessa, or FACS SCAN flow cytometers (BD Biosciences), and data analyzed using FlowJo.

Real time RT-PCR analysis. Total RNA was prepared using a QIAGEN RNeasy mini kit with on-column DNase digestion, or using TriPure (Roche) according to the manufactures protocol, followed by reverse transcription using Superscript II (Invitrogen). Quantitative PCR was carried out on a Roche Lightcycler 480 using Lightcycler 480 SYBR Green Master mix (Roche). Relative quantification was carried out using Gapdh as a reference gene. All PCRs were carried out in triplicate, and the mean crossing point was used for quantification. Primer sequences were designed such that they spanned splice junctions whenever possible and are provided in Table S3.

Immunohistochemistry. Cells were fixed with 4% paraformaldehyde for 10 min at 4°C, permeabilized for 10 min with ice-cold methanol, washed with PBS/0.5% Triton X-100 (PBT), and blocked with 1% BSA (Sigma) and 5% normal donkey serum in PBT (blocking solution) for 1 hour. Samples were then incubated with primary antibody in blocking solution overnight at 4°C, washed three times with PBT, and primary antibodies detected by DyLight-488 or -594 labelled secondary antibodies (Jackson ImmunoResearch), followed by imaging. Antibodies and concentrations: goat-anti-Oct4 (Santa Cruz sc-8628, 1:250), rabbit-anti-Nanog (REC-RCAB0002P-F Cosmo Bio, 1:250), rabbit-anti-T (Santa Cruz sc-20109, 1:100), goat-anti-T (Santa Cruz sc-17743, 1:100) and rabbit-anti-Gata4 (Santa Cruz sc-9053, 1;100), goat-anti-Sox2 (Immune Systems, 1:1000), rabbit-anti- E-cadherin (Cell Signaling 24E10, 1:200), rabbit-anti-Neuronal Class III B-tubulin (Covance PRB-435P, 1:500), mouse-anti-Cdx2 (Biogenex, MU392A-UC 1:400). Human ESCs were stained for alkaline phosphatase according to manufacturer's protocol (Millipore, Alkaline Phosphatase Detection Kit SCR004).

X-gal staining. Embryos were fixed for 30 min and cells for 1 min in 0.5% glutaraldehyde and 1% paraformaldehyde in PBS, washed in PBS and incubated in X-Gal solution composed of 0.1% 5-Bromo-4-chloro-3-indolyl β-D-galactopyranoside, 0,02% Nonidet™ P 40, 0.01% Sodium Deoxycholate, 2mM magnesium chloride, 5mM potassium hexacyanoferrate(III), 5mM potassium hexacyanoferrate(II) trihydrate, 1mM ethylene glycol-bis(2-aminoethylether)-*N,N,N′,N′*-tetraacetic acid (all from Sigma) for 5 h to overnight at room temperature. Stained cells were counterstained with neutral red and photographed with an Olympus BX40 light microscope.

Micro-array analysis. Total RNA was prepared using TriPure (Roche) according to the manufacturer's protocol from GFP9 EpiSCs maintained in the presence or absence of IWP2 for 2 passages in EpiSC medium. RNA was converted to biotin-labeled cRNA, hybridized on the Affymetrix Mouse Genome 430 2.0 Array, and analyzed with the Affymetrix GeneChip Scanner 3000 at the Erasmus MC Center for Biomics (Rotterdam, The Netherlands) according to manufacturer's instructions. Raw intensity values were normalized by calling Variance

Stabilization (VSN) and calculating the summaries with the medianpolish algorithm of the Robust Multi-Array Average (RMA) expression (Huber et al., 2002; Irizarry et al., 2003). The probe sets gene annotations were based on Ensembl release 75 (Flicek et al., 2014). Quality control was investigated using the *qc* function from the *simpleaffy* R package. Differentially expressed genes were called with the *limma* package, using a threshold value of 0.05 for False Discovery Rate (FDR) adjusted p-value and minimal fold change of 2.
Gene Set Enrichment Analysis (Subramanian et al., 2005) was run on the vehicle versus IWP treated EpiSCs, with 1000 permutations per run. Permutation type was set to "phenotype". The enrichment statistic used was weighted and signal to noise was used as our preferred metric for gene ranking.
To combine gene expression data from Affymetrix GeneChip and Illumina BeadArray platforms, we used a similar approach as described previously (Heider and Alt, 2013). We first downloaded 112 gene expression datasets deposited in the Gene Expression Omnibus (GEO) database (GSE46227) (Kojima et al., 2014) and combined these data with our 9 Affymetrix GeneChip datasets. The probes and probesets were combined using the probe(set)s/gene annotation of Ensembl release 75 (Flicek et al., 2014). In each sample, genes with multiple probe/probesets were collapsed to their median value. This resulted in 17058 distinct genes from both platforms. Second, we quantile normalized the combined expression data (Bolstad et al., 2003). Third, we applied the Empirical Bayes method (Johnson et al., 2007) in a unsupervised mode using the CrOss-platform NOrmalization in R (CONVOR) package (Rudy and Valafar, 2011). We verified the proper unsupervised hierarchical clustering with euclidean distance of the cross-platform normalized data (data not shown). Subsequently we selected the gene expression values from EpiSCs and Epiblast/Ectoderm samples cultured in Tam's and our lab to conduct a Principal Component Analysis (PCA). Using R, the PCA was calculated based on the covariance matrix of 1117 genes that are differentially expressed with a FDR <0.05 and a fold change of at least 1.5.
RNA Seq. Total RNA was prepared using TriPure (Roche) according to the manufacturer's protocol from GFP9 EpiSCs treated for 48 hrs with Bmp4, Wnt3a, and/or IWP2 in EpiSC medium. RNA-Seq was performed at the Erasmus MC Center for Biomics (Rotterdam, The Netherlands) according to manufacturer's instructions (Illumina). Briefly, polyA containing mRNA molecules were purified using poly-T oligo attached magnetic beads. Following purification, the mRNA was fragmented into ~200 bp fragments using divalent cations under elevated temperature. The cleaved RNA fragments were copied into first strand cDNA using reverse transcriptase and random primers. This was followed by second strand synthesis using DNA polymerase I and RNaseH treatment. These cDNA fragments were end repaired, a single A base was added and Illumina adaptors were ligated. The products were purified and size selected on gel and enriched by PCR. The PCR products were purified by Qiaquick PCR purification and used for cluster generation according to the Illumina cluster generation protocols (www.illumina.com). The sample was sequenced for 36bp and raw reads were uploaded on the Galaxy main server (www.usegalaxy.org) (Goecks et al., 2010) and a standard pipeline for RNA-Seq analysis was applied, using modules from the Tuxedo suite. Samples were filtered and trimmed with FASTQ. The resulting files were aligned to the mm9 reference genome build using preSet settings. The aligned reads were imported to Cufflinks, using multi-read and effective length correction, and FPKM values calculated. The mm9 build was used as a reference annotation. Principal component analysis on the FPKM values was performed using Tibco Spotfire on the 9939 genes that had a FPKM value of 5 or more in at least one of the 4 samples.

PCR primer sequences		
Mouse	**Forward**	**Reverse**
Gapdh	TATGATGACATCAAGAAGGTGG	CATTGTCATACCAGGAAATGAG
Oct4	GAACATGTGTAAGCTGCGG	CAGACTCCACCTCACACG
Sox2	AGCTCGCAGACCTACATGAA	CCCTGGAGTGGGAGGAA
Nanog	AAAGGATGAAGTGCAAGCG	TCTGGCTGCTCCAAGTT
Fgf5	AATATTTGCTGTGTCTCAGG	TAAATTTGGCACTTGCATGG
Otx2	CATGATGTCTTATCTAAAGCAACCG	GTCGAGCTGTGCCCTAGTA
Dnmt3b	CCAAGGACACCAGGACGCGC	TCCGAGACCTGGTAGCCGGAA
Rex1	GCTCCTGCACACAGAAGAAA	GTCTTAGCTGCTTCCTTCTTGA
Pecam1	CAAAGTGGAATCAAACCGTATCT	CTACAGGTGTGCCCGAG
Stella	TTCAAAGCGCCTTTCCCAA	ACATCTGAATGGCTCACTG
Wnt1	ATGAACCTTCACAACAACGA	GGCGATTTCTCGAAGTAGAC
Wnt2b	CATGAACTTACACAACAACC	CAAAGTAGACAAGATCAGTCC
Wnt3	CAAGCACAACAATGAAGCAG	GGAGTTCTCGTAGTAGACCA
Wnt3a	AGTGAGGACATTGAATTTGG	GTTTCTCTACCACCATCTCC
Wnt4	GAATCTTCACAACAACGAGG	ATCTGTATGTGGCTTGAACTG
Wnt5a	TAATTCTTGGTGGTCTCTAGGT	GCACCTTCTCCAATGTACTG
Wnt5b	TATGCAGATAGGTAGCCGAG	TTGTTCTGTAGGTTCATGAGAG
Wnt7a	CATCATCGTCATAGGAGAAGG	GATAATCGCATAGGTGAAGG
Wnt7b	CATGAACCTTCACAACAATGAG	TTGTACTTCTCCTTGAGCAG
Wnt8b	GTACACCCTGACTAGAAACTG	ATTGTTGTGCAGATTCATGG
Wnt9a	AGTACAGCAGCAAGTTTGTC	GAGCGAGGTCTCATATTTGTG
Wnt10b	CGGGATTTCTTGGATTCCAG	TTGTGGGTATCGATAAAGATGG
Wnt11	GATCCCAAGCCAATAAACTG	AGATACACAAGTTCTGAGTCCT
Wnt16	CTCTTTGGCTATGAGCTGAG	CGTTGTTGTGTAGATTCATGG
T	GAACCTCGGATTCACATCG	GGCATCAAGGAAGGCTTTAG
Sp5	CGGGACCTATGAGCGCA	TTCGGGCGGAGGAGAAT
Sox17	TGTATGAGTTCTTTGGAGACAAAGTAG	ATAGGAAGGCTGAAATTCAGATG
Snail1	CTTGTGTCTGCACGACCTGT	CTTCACATCCGAGTGGGTTT
Klhl4	CAACAACTGCCACTCCAAATTG	TATGGATGCTGCTAAAGGCAC
Zfp42	TCGGGGCTAATCTCACTTTCAT	CCCTCGACAGACTGACCCTAA
Prdm14	AGCACCCAACCGACTTACAG	GTGGCACATCACCAAATGAG
Tbx3	CAGCAGCCCCCACTAACTG	AGATCCGGTTATCCCTGGGAC
Pou3f1	GGCGCATAAACGTCGTCCA	TCGAGGTGGGTGTCAAAGG
Lefty1	CGCGAAACGAACCAACTTGT	CCAACCGCACTGCCCTTAT
Pitx2	GTCCGTGAACTCGACCTTTTT	GCAGCCGTTGAATGTCTCTTC
Lrp2	GGCTGCATACATTGGGTTTTCA	AAAATGGAAACGGGGTGACTT
Slc39a8	GCCTAAGCATCCAGAGGGAGA	CAGGTATGTCCTGCTGATTGC
Prss23	GGCGTCGAAGTCTGCCTTAG	GGTGAGTCCCTACACCGTTC
Klhl4	CAACAACTGCCACTCCAAATTG	TATGGATGCTGCTAAAGGCAC
Spry4	TCTGGTCAATGGGTAAGATGGT	GCAGCGTCCCTGTGAATCC
Thbs1	CGGGGATCAGGTTGGCATT	GGGGAGATAACGGTGTGTTTG
Fn1	GCCCAGTGATTTCAGCAAAGG	ATGTGGACCCCTCCTGATAGT
Kit	GTCGCCAGCTTCAACTATTAACT	GCCACGTCTCAGCCATCTG
Map2k6	TTGGAGTCTAAATCCCGAGGC	ATGTCTCAGTCGAAAGGCAAG
Fgf15	CTGACACAGACTGGGATTGCT	ATGGCGAGAAAGTGGAACGG
Epas1	TGTGTCCGAAGGAAGCTGATG	CTGAGGAAGGAGAAATCCCGT
Rhox5	CCCTGGTGCCACTATCCTT	ACTCGGAAGAACAGCATGATG
Fgf4	GCTGCTCATAGCCACGAAGAA	GGGCATCGGATTCCACCTG
Klf2	CACGTTGTTTAGGTCCTCATCC	CTCAGCGAGCCTATCTTGCC
Alpl	GGCTACATTGGTGTTGAGCTTTT	CCAACTCTTTTGTGCCAGAGA
Tnfrsf19	AGAAAATTCAGCGCAGATGGAA	TTCTGTGGGGGACACGATG
Krt8	ATCGAGATCACCACCTACCG	TGAAGCCAGGGCTAGTGAGT
Krt19	TGACCTGGAGATGCAGATTG	AATCCACCTCCACACTGACC
Nedd9	CCACAGCACTCAAGGGGTAT	ATGGTGGAATGGCATAGACC
Plat	AGTGGTCTTGGGCAGAACAT	CTGCAGTAATGCGATGTCGT

Mnx1	GTTGGAGCTGGAACACCAGT	CTTTTTGCTGCGTTTCCATT
Lgr5	TAACAGGGAACCGAGCCTTA	CACTGTTGCCGTCGTCTTTA
Vil1	CTGGAAACCGAGACCTTGAG	AGTTTCCCAGCTCTGCCTTA
Fgf8	CCGGACCTACCAGCTCTACA	ACTCGGACTCTGCTTCCAAA
Id1	GAGTCTGAAGTCGGGACCAC	GAGTCCATCTGGTCCCTCAG
Cdh2	GGGGATATTGGGGACTTCAT	GAGTTGAGGGAGCTCAAGGA
Plet1	CTTGACATCCCAAAGCCAGT	GGTTGAGGCTGAGGTTGTA
Cdh1	GCCACCAGATGATGATACCC	GGAGCCACATCATTTCGAGT
Nodal	ACCATGCCTACATCCAGAGC	CATGTCCTTGTGGTGTTCCA
Axin2	AGGAGCAGCTCAGCAAAAAG	GCTCAGTCGATCCTCTCCAC
Human	**Forward**	**Reverse**
GAPDH	GGCCTCCAAGGAGTAAGACC	AGGGGTCTACATGGCAACTG
BRY	GCAAAAGCTTTCCTTGATGC	ATGAGGATTTGCAGGTGGAC
HOXB1	TCCCTGGGAACTTTGACAAC	GCTCTGACACCTTCGCTAGG
WNT3	GCTGACTTCGGCGTGTTAGT	CACTTGCATTTGAGGTGCAT
POU5F1	CGAAAGAGAAAGCGAACCAG	ACACTCGGACCACATCCTTC
KRT7	CAGGAACTCATGAGCGTGAA	CTGCCACCAGTGGAATTCAT
ENPEP	AAGAACATGGCCTGGAATTG	AGCTCTCCATCTGCCACAGT
GCM1	CCTCTGAAGCTCATCCCTTG	GCTCTTCTTGCCTCAGCTTC
SOX2	AACCCCAAGATGCACAACTC	CGGGGCCGGTATTTATAATC
NANOG	CAGAAGGCCTCAGCACCTAC	ACTGGATGTTCTGGGTCTGG
T	TCGGAACAATTCTCCAACCT	GGGTACTGACTGGAGCTGGT
MIXL1	AGTCCAGGATCCAGGTATGGT	GGGGCTTCAGACATTTCGT
FOXA2	GAGGGCTACTCCTCCGTGA	CACGTACGACGACATGTTCA
CGA	GGTGCCCCAATACTTCAGTG	CCCCATTACTGTGACCCTGT
SOX17	AGCAGAATCCAGACCTGCAC	TTGTAGTTGGGGTGGTCCTG
SIX3	CGGGAGTGGTACCTACAGGA	GGTGCTGGAGCCTGTTCTT
HESX1	TAGAGGCCGAAGACCAAGAA	ACGCCGATTTTGAAACCA
FOXD3	ACTCTGCCTCTCCCCAATTT	TCGGTTTTCGGTTTTACCTG
SOX1	AAAGTCAAAACGAGGCGAGA	AAGTGCTTGGACCTGCCTTA
PAX6	GCCAGCAACACACCTAGTCA	TGTGAGGGCTGTGTCTGTTC
ASCL1	GGACGAGGGCTCTTACGAC	AACGCCACTGACAAGAAAGC

Supplemental References

Bernemann, C., Greber, B., Ko, K., Sterneckert, J., Han, D.W., Arauzo-Bravo, M.J., and Scholer, H.R. (2011). Distinct developmental ground states of epiblast stem cell lines determine different pluripotency features. Stem cells (Dayton, Ohio) *29*, 1496-1503.

Bolstad, B.M., Irizarry, R.A., Astrand, M., and Speed, T.P. (2003). A comparison of normalization methods for high density oligonucleotide array data based on variance and bias. Bioinformatics *19*, 185-193.

Drukker, M., Tang, C., Ardehali, R., Rinkevich, Y., Seita, J., Lee, A.S., Mosley, A.R., Weissman, I.L., and Soen, Y. (2012). Isolation of primitive endoderm, mesoderm, vascular endothelial and trophoblast progenitors from human pluripotent stem cells. Nature biotechnology *30*, 531-542.

Flicek, P., Amode, M.R., Barrell, D., Beal, K., Billis, K., Brent, S., Carvalho-Silva, D., Clapham, P., Coates, G., Fitzgerald, S.*, et al.* (2014). Ensembl 2014. Nucleic Acids Res *42*, D749-755.

Goecks, J., Nekrutenko, A., Taylor, J., and Galaxy, T. (2010). Galaxy: a comprehensive approach for supporting accessible, reproducible, and transparent computational research in the life sciences. Genome biology *11*, R86.

Greber, B., Wu, G., Bernemann, C., Joo, J.Y., Han, D.W., Ko, K., Tapia, N., Sabour, D., Sterneckert, J., Tesar, P.*, et al.* (2010). Conserved and divergent roles of FGF signaling in mouse epiblast stem cells and human embryonic stem cells. Cell stem cell *6*, 215-226.

Heider, A., and Alt, R. (2013). virtualArray: a R/bioconductor package to merge raw data from different microarray platforms. BMC Bioinformatics *14*, 75.

Hsieh, J.C., Rattner, A., Smallwood, P.M., and Nathans, J. (1999). Biochemical characterization of Wnt-frizzled interactions using a soluble, biologically active vertebrate Wnt protein. Proceedings of the National Academy of Sciences of the United States of America *96*, 3546-3551.

Huber, W., von Heydebreck, A., Sultmann, H., Poustka, A., and Vingron, M. (2002). Variance stabilization applied to microarray data calibration and to the quantification of differential expression. Bioinformatics *18 Suppl 1*, S96-104.

Irizarry, R.A., Hobbs, B., Collin, F., Beazer-Barclay, Y.D., Antonellis, K.J., Scherf, U., and Speed, T.P. (2003). Exploration, normalization, and summaries of high density oligonucleotide array probe level data. Biostatistics *4*, 249-264.

Johnson, W.E., Li, C., and Rabinovic, A. (2007). Adjusting batch effects in microarray expression data using empirical Bayes methods. Biostatistics *8*, 118-127.

Kojima, Y., Kaufman-Francis, K., Studdert, J.B., Steiner, K.A., Power, M.D., Loebel, D.A., Jones, V., Hor, A., de Alencastro, G., Logan, G.J.*, et al.* (2014). The transcriptional and functional properties of mouse epiblast stem cells resemble the anterior primitive streak. Cell stem cell *14*, 107-120.

Okabe, M., Ikawa, M., Kominami, K., Nakanishi, T., and Nishimune, Y. (1997). 'Green mice' as a source of ubiquitous green cells. FEBS Lett *407*, 313-319.

Rudy, J., and Valafar, F. (2011). Empirical comparison of cross-platform normalization methods for gene expression data. BMC Bioinformatics *12*, 467.

Soriano, P. (1999). Generalized lacZ expression with the ROSA26 Cre reporter strain. Nature genetics *21*, 70-71.

Subramanian, A., Tamayo, P., Mootha, V.K., Mukherjee, S., Ebert, B.L., Gillette, M.A., Paulovich, A., Pomeroy, S.L., Golub, T.R., Lander, E.S.*, et al.* (2005). Gene set enrichment analysis: a knowledge-based approach for interpreting genome-wide expression profiles. Proceedings of the National Academy of Sciences of the United States of America *102*, 15545-15550.

Willert, K., Brown, J.D., Danenberg, E., Duncan, A.W., Weissman, I.L., Reya, T., Yates, J.R., 3rd, and Nusse, R. (2003). Wnt proteins are lipid-modified and can act as stem cell growth factors. Nature *423*, 448-452.